December 2018

# Synthesis and Performance Analysis of Polyethersulfone (PES) Nanocomposite Membrane Grafted with Functionalized Iron (II, III) Oxide Nanoparticles for Arsenate Removal

JIYOUNG ROWLEY
*University of Wisconsin-Milwaukee*

# SYNTHESIS AND PERFORMANCE ANALYSIS OF POLYETHERSULFONE (PES) NANOCOMPOSITE MEMBRANE GRAFTED WITH FUNCTIONALIZED IRON (II, III) OXIDE NANOPARTICLES FOR ARSENATE REMOVAL

by

Jiyoung Rowley

A Thesis Submitted in
Partial Fulfillment of the
Requirements for the Degree of

Master of Science
in Engineering

at
The University of Wisconsin-Milwaukee
December 2018

# ABSTRACT

## SYNTHESIS AND PERFORMANCE ANALYSIS OF POLYETHERSULFONE (PES) NANOCOMPOSITE MEMBRANE GRAFTED WITH FUNCTIONALIZED IRON (II, III) OXIDE NANOPARTICLES FOR ARSENATE REMOVAL

by

Jiyoung Rowley

The University of Wisconsin-Milwaukee, 2018

Under Supervision of Professor Nidal H Abu-Zahra

Arsenic (As) is one of the detrimental elements in nature, which has negative effect on human health as well as the environment. High levels of arsenic concentration in the drinking water can cause skin, bladder, lung liver, and prostate, as well as cardiovascular, pulmonary, immunological, neurological and endocrine diseases. Arsenic pollution in the water has been reported in many countries as a worldwide problem, including the United States.

To develop a separation method for removing Arsenic, various treatment technologies including precipitation, coagulation with ferric chloride or aluminum sulfate coagulants, ion exchange and adsorption with modified nanocomposite material have been extensively studied. All these methods have drawbacks in terms of costs and efficiencies by the generation of toxic sludge in coagulation and precipitation method and causing severe pressure drops in column

adsorption process and high cost of operation in ion exchange. However, membrane technology, which has drawn considerable attention in the past few decades by offering a promising solution for water treatment and pollutant separation. Among the pressure driven membranes, especially nanofiltration (NF) and reverse osmosis (RO) are widely used for arsenic removal even though the process requires high operational pressure and costly membranes comparing with low pressure processes such as microfiltration (MF) and ultrafiltration (UF). In the case of removing small size pollutants such as arsenate, microfiltration (MF) and ultrafiltration (UF) membranes can overcome these disadvantages by the incorporation of Nano inorganic particle absorbents in the polymer matrix membranes.

In this research work, functionalized Iron Oxide nanoparticles (APTES-$Fe_3O_4$) were impregnated into a Polyethersulfone(PES) membrane in order to remove arsenic by exploiting the PES membranes inherent filtration capability and reaction between the Iron oxide compounds and arsenic species by adsorption mechanism, which provides high As(V) removal capacity. APTES(Aminopropyltriethoxysilane) was reacted with Iron Oxide NPs to modify their surface for generating strong repulsion between NPs. The modification also prevents those nano particles' aggregations and leads to good dispersion in the PES membrane matrix.

To characterize the modification of NPs with APTES (A-$Fe_3O_4$ NPs), Infrared Spectroscopy was utilized to verify the surface modification of $Fe_3O_4$ NPs. TGA analyzed the degree of dispersity of A-$Fe_3O_4$ NPs in PES membrane matrix. Pore structure of prepared membrane was characterized by FESEM and surface roughness was measured with AFM (Atomic Force Microscopy). Porosity and mean pore radius size were calculated with gravimetric method by using the weight difference of wet and dry membranes. Mean pore size was gained by Guerout-Elford-Ferry equation with water flux volume and pressure drop. For

analyzing As(V) ion removal capacity through ion concentration of the permeate, ICP-MS method was utilized.

To evaluate the As(V) removal performance difference and find the best rejection of As(V), pure PES membrane was developed by adding APTES-Fe3O4 NPs in different weight percentages (1, 2, 3wt %). Batch adsorption tests were conducted with different As(V) concentration solution (2ppm, 4ppm, 6ppm, 8ppm) to study isotherm model. Kinetic adsorption experiments for As(V) removal were conducted in 50mL membrane cell under 50psi pressure with 1ppm As(V) solution for better understanding of adsorption process mechanism.

It was confirmed that A-Fe3O4 NPs were dispersed in good quality with the residual weight percent from TGA value. Moreover, FESEM images and AFM results indicated that PES containing 1wt%, 2wt% and 3wt% of A-Fe3O4 NPs tends to have more porous structure and higher roughness on the surface that pure PES membrane.

Higher percentage of pores over 60% was shown with PES containing more A-$Fe_3O_4$ NPs. Sub-layer micro-void is inclined to be formed in a bigger size with the addition of A-Fe3O4 NPs. This increased micro-void size in the bottom layer affected critically on pure water flux value. The larger the pore structure with A-$Fe_3O_4$ NPs, the prepared membrane showed better performance for the pure water flux by having the highest value 23.9$Lm^{-2}h^{-1}bar^{-1}$ (in the case of M4). Furthermore, hydrophilicity was characterized with water contact angle. These values indicated the range between 61˚and 76˚. Lowest contact angle was found in the PES containing 3wt % A-$Fe_3O_4$.

From the batch adsorption test results, sorption isotherm models were applied to define the equilibrium adsorption capacities of membranes with different concentration of As(V)

solutions. Freundlich and Langmuir models were well fitted into data by giving $R^2$ as 0.9996 and 0.9955 in PES-A-$Fe_3O_4$ NPs 3wt% membrane, respectively. Mostly, Langmuir model gives higher $R^2$ for the linear regression of the prepared membranes.

Dynamic adsorption results gained under pressure, 50psi in a 50mL membrane cell showed the highest rejection percentage, 76% from PES-A-$Fe_3O_4$ NPs 3wt% membrane. Most of nanocomposites with A-$Fe_3O_4$ NPs were equilibrated at 270mins.

The prepared PES membrane nanocomposite in this research proves its high capability to remove arsenate with its good thermal stability and resistance to extreme pH conditions. Physical separation through membrane, in addition to adsorption behavior of PES can propose this PES-A-$Fe_3O_4$ NPs membrane to be an efficient medium for removing As(V) from aqueous solution.

# TABLE OF CONTENTS

**ABSTRACT** ..... ii

**LIST OF FIGURES** ..... ix

**LIST OF TABLES** ..... xii

**ACKNOWLEDGEMENTS** ..... xiii

**CHAPTER 1** ..... 1

**1.1. Arsenic** ..... 2
1.1.1. Arsenic Chemistry ..... 2
1.1.2. Arsenic Sources ..... 4
1.1.3. Arsenic Toxicity ..... 6
**1.2. Separation Method for Removal of Arsenic** ..... 8
1.2.1. Adsorption and Ion Exchange Method ..... 8
1.2.2. Precipitative/Coprecipitation Method ..... 10
1.2.3. Membrane Method ..... 12
1.2.4. Biological treatment Method ..... 13
1.2.5. Emerging treatment Method ..... 15
1.3 **Polyethersulfone(PES) Membrane: An Overview** ..... 17
1.4 **Literature Review: Arsenic Removal from Water** ..... 22
**1.5 Research Objectives** ..... 28

**CHAPTER2** ..... 29

**2.1 Materials** ..... 29
2.1.1 Polyetheruslfone(PES) ..... 29
2.1.2 Polyvinylpyrrolidone(PVP) ..... 30
2.1.3 N, N-dimetylacetamide(DMAc) ..... 31
2.1.4 Iron Oxide Nano Particles($Fe_3O_4$-NP) ..... 33
2.1.5 Aminopropyltriethoxysilane(APTES) ..... 34
**2.2 Synthesis and Characterization** ..... 35
2.2.1 Synthesis of PES Nanocomposite Membrane ..... 35
2.2.2 Synthesis of $Fe_3O_4$-NP grafted APTES ..... 37
2.2.3 Characterization of $Fe_3O_4$-NP grafted with APTES ..... 38
2.2.4 Characterization of PES Nanocomposite Membrane ..... 39
**2.3 Membrane Filtration and Adsorption Experiments** ..... 42

**CHAPTER3** ..... 47

**3.1Characterization Analysis** ..... 47
3.1.1 FESEM Analysis ..... 47
3.1.2 Thermal Analysis(TGA) ..... 49
3.1.3 Atomic Force Microscopy(AFM) and Porosity ..... 51
3.1.4 Contact Analysis ..... 53
3.1.5 IR Analysis ..... 55
3.1.6 TEM Analysis ..... 58

**3.2 Performance Analysis** ..... 59
3.2.1 Water Flux of Membranes ..... 59
3.2.2 Arsenic Adsorption of Membrane ..... 60
CHAPTER4 ..... 65
REFERENCES ..... 68

# LIST OF FIGURES

**Figure 1.1** Speciation of arsenic acid with pH. [10] ..... 3

**Figure 1.2** Map showing significant arsenic contamination problems in the United States [17] . 5

**Figure 1.3** Iron Oxide Power [30] ..... 10

**Figure 1.4** A typical precipitation/coprecipitation system [25] ..... 11

**Figure 1.5** **Left** : Ultrafiltration by pressure **Right** : Reverse Osmosis [39] ..... 12

**Figure 1.6** Three-compartment electro dialysis cell and scheme of the ions transport [40] ..... 13

**Figure 1.7** Molecular structure of Polysulfone and Polyethersulfone [54] ..... 17

**Figure 1.8** Share of global consumption of polyarylsulfone thermoplastics by application area (2012) [60] ..... 19

**Figure 1.9** Cross-sectional SEM images of the prepared PES membrane.(Pristine) [64] ..... 20

**Figure 1.10** Cross-sectional view of an asymmetric membrane. [65] ..... 21

**Figure 1.11** (a) residual arsenic concentration and (b) percentage arsenic removal [66] ..... 22

**Figure 1.12** (a) Arsenate isotherm curves for Darco 20×50 Fe-GACs (lines are the Langmuir model fits). ..... 23

**Figure 1.13** Arsenic removal as a function of pH by adsorption on various iron oxide mineral [68-71] ..... 25

**Figure 1.14** Concentration dependent adsorption kinetics of As(III) ions using Fe3+ incorporated ..... 26

**Figure 2.1** Polyethersulfone chemical structure [54] ..... 29

**Figure 2.2** Chemical Structure of Polyvinylpirrolidone(PVP) [79] ..... 31

**Figure 2.3** Chemical Structure of N, N- Dimethylacetamide (DMAc) [82] ..... 32

**Figure 2.4** FE-TEM images of the iron oxide nanoparticles (Magnetite and maghemite)

(A) Scale bar: 50nm. (B) Scale bar: 100nm. [88] ..... 33

**Figure 2.5** Chemical Structure of Aminopropyltriethoxylsilane [91] ..... 35

**Figure 2.6** Experimental setup for dissolving PES pellet in DMAc ..... 136

**Figure 2.7** Experimental setup for modification of Fe3O4-NPs with APTES..... 37

**Figure 2.8** Silanization of magnetic iron oxide nanoparticles with APTES [90] ..... 38

**Figure 2.9** Experimental Sep-up used for Arsenate (As) removal from solutions. ..... 43

**Figure 2.10** Experimental Set-up for Batch adsorption tests ..... 44

**Figure 2.11** Schematic representation of the essential parts of mass spectrometric

instrumentation [98] ..... 46

**Figure 3.1** Cross-sectional FESEM images of the prepared membranes, (a) M1: Pristine PES, (b)

M2: PES-A-Fe3O4 1wt%, (c) M3: PES-A-Fe3O4 2wt%, (d) M4: PES-A-Fe3O4 3wt%. ..... 48

**Figure 3.2** FESEM Image of cross section of M2(left) and M4(right) ..... 49

**Figure 3.3** TGA for M2, M3, M4 APTES-Fe3O4 NPs dispersion .....50

**Figure 3.4** Two dimensional(2D) AFM Image (a) M1, (b) M2, (c) M3, (d) M4..... 51

**Figure 3.5** Three dimensional(3D) AFM Image (a) M1, (b) M2, (c) M3, (d) M4..... 52

**Figure 3.6** Average Water Contact Angle of PES-A-Fe3O4 NPs membrane (0, 1, 2, 3wt. %)... 54

**Figure 3.7** Image from Goniometer for Water Contact Angle of each membrane sample. (a)

Pristine PES, (b) PES-A-Fe3O4 1wt%, (c) PES-A-Fe3O4 2wt%, (d) PES-A-Fe3O4 3wt%..... 55

**Figure 3.8** IR spectra of unmodified (a) and APTES modified (b)..... 56

**Figure 3.9** Chemical structure of silane coupling agent (APTES) [91] ..... 56

**Figure 3.10** IR spectroscopy for (a) Original PES and (b) PES-1wt% APTES-Fe3O4..... 57

**Figure 3.11** Figure 3.11 TEM Images for APTES-Fe3O4 NPs ..... 58

**Figure 3.12** Pure water permeability (PWP) of the prepared each sample (M1, M2, M3, M4) .. 59

**Figure 3.13** Equilibrium adsorption curves of As(V) : Qe..... 60

**Figure 3.14** Langmuir adsorption isotherm of nanocomposite membranes, conditions: T=25° C, pH=2 ..... 62

**Figure 3.15** Freundlich adsorption isotherm of nanocomposite membranes, T=25° C, pH=2 ... 62

**Figure 3.16** Prepared Membranes (M2, M3, M4) As(V) ion Permeate Concentration at 50psi.. 64

**Figure 3.17** Prepared Membranes (M2, M3, M4) As(V) ion rejection at 50psi ..... 64

# LIST OF TABLES

**Table 1.1** Chronic and acute effects of being exposed to inorganic arsenic ..... 7

**Table 1.2** Iron coated/g polystyrene as affected by the initial concentration of ferric nitrate [66] ..... 22

**Table 2.1** Weight Concentration of chemical components in each PES sample..... 34

**Table 2.2** List of characterizations and purpose of each ..... 46

**Table 3.1** Expected A-Fe3O4 and experimental A-Fe3O4 from TGA residual ..... 50

**Table 3.2** Roughness parameters, porosity, and mean porous radius of membranes..... 53

**Table 3.3** Langmuir and Freundlich isotherm parameters for As(V) removal using nanocomposite membranes with different APTES-Fe3O4 contents pH=2 ..... 63

# ACKNOWLEDGMENTS

In the first place, I express my deepest gratitude and appreciations to my advisor, Dr. Nidal Abu-Zahra. I have been amazingly privileged to have an advisor who gave me chance to explore on my own and guided me when my research project faced obstacles. Thank you for your support to get this work done and giving me the chance to be grown up as a researcher in graduate school. I would not forget your favor for me to accomplish this research goal in my whole life.

I am grateful for Dr. Benjamin Church and Dr. Anna Benko for being in my examination committee. Thank you for your time, as well as, your advice and encouragements I earned from both of you while I was working in this research project. I extend my gratefulness to all academic staff, colleagues, and friends I have known in UW-Milwaukee. Without their help, none of my accomplishment could be possibly achieved.

At the end, I cannot express how much I am in gratitude and grateful to my parents (Seong Keun, Nam Yeon) in South Korea. Both of you have encouraged me by believing in my abilities. I would like to express my love and my thankfulness to my husband, Colin Rowley who believes in my ambition and supported me all the time throughout this long journey. I made this journey successful eventually because you were with me anytime and anywhere.

# CHAPTER1
# INTRODUCTION

Contamination of drinking water by heavy metal ions such as Arsenic has been considered as a serious problem locally and globally with environmental and physiologically harmful effects on human beings and other living creatures. There have been many great efforts in research projects to treat the detrimental metal ions by developing efficient methods such as separation, absorption, precipitation and other emerging technologies. In this research, Polyethersulfone(PES) membrane added with modified Iron Oxide Nano particle were studied for removing arsenic through filtration (Membrane) and adsorption (modified Nano particle).

In this thesis outline, the following description can show it in the following order. In the first chapter, five sections contain overall information which will be utilized for developing the research experiments and gaining the expected results. The information about arsenic, the treatment and separation method such as adsorption, ion exchange, membrane filtration, precipitation, biological treatment, and other emerging techniques were described. The following parts are about molecular structure and properties of Polyethersulfone membrane and literature review about removal of arsenic through membrane. Last part explains about my research plan and final objectives that I have aimed at for the whole process.

In chapter 2, the experimental setup for membrane synthesis and nano particle treatment are presented. The raw materials, experimental setup, synthesis and characterization of membrane with nanoparticles are specifically explained in this order. In chapter 3, the results of membrane or nanoparticle characterization and its performance for arsenic removal are shown. The final chapter 4 includes the conclusions drawn mainly from chapter 3 experimentations.

## 1.1 Arsenic

### 1.1.1 Arsenic Chemistry

Arsenic is a group 15 element on the periodic table along with nitrogen, phosphorus, antimony, and bismuth. The atomic mass of arsenic is around 75 amu, which has nucleus of isotope containing 42 neutrons and 33 protons. Numerous artificial short-lived radioisotopes of arsenic have been produced, including excited-state isomers. [1] An arsenic atom in a covalent bond shares its valence electrons with another atom in the bond. But, the valence electron in a covalent bond are not equally shared between the arsenic atom and the atom of the other element. This property leads to the phenomena that the most of the covalent bonds in arsenic atom still have an ionic character. [2] The most common valence states of arsenic are -3, 0, +3, and +5. Like sulfide in sulfide in pyrite, arsenic in arsenic-rich(arsenian) pyrite($FeS_2$), arsenide and arseno-sulfide minerals have a valence state of -1 or 0. In arsenide niccolite(NiAs), every nickel atom is surrounded by six arsenic atoms, where arsenic has a valence state of -1 and nickel is +1 [3-5] Arsenic dissolved in natural waters is predominantly in as the form of +3 and +5. $As^{3+}$ and $As^{5+}$ usually bond with oxygen to form inorganic arsenite (inorganic As(III)) and arsenate (inorganic As(V)), respectively.

As(III) mostly exists in low-oxygen(reducing) groundwaters and hydrothermal waters. Although As(V) is usually the prominent from of arsenic in toxic waters, biological activity may result in significant concentrations of metastable As(III) and even mildly reducing conditions in groundwater usually results in more As(III) than As(V). [6] As fluids approach the surface and become diluted with aerated groundwater, As(III) will begin to oxidize to As(V). By itself, air is very slow in oxidizing As(III) and considerable As(II) may persist for some time even under

well-aerated conditions In surface and near-surface environments, natural chemicals, light, and/or microbial activity can increase the oxidation of As(III).[7-9]

In anoxic groundwater and other reducing waters, inorganic arsenite (As(III)) commonly hydrates to arsenious acid, which primarily exists as dissolved $H_3AsO_3^0$ at pH conditions below 9.2 and as its dissociated anions ($H_2AsO_3^-$, $HAsO3^{2-}$, and $AsO3^{3-}$) under alkaline conditions. However, the dominant form of arsenic in oxic natural waters is usually dissolved arsenic acid, which includes $H_3AsO_4^0$ under very acidic (pH < 2) conditions and its associated anions ($H_2AsO_4^-$, $HAsO_4^{2-}$, and/or $AsO_4^{3-}$) in less acidic, neutral, and alkaline waters. [10] Figure 1.1 shows the calculated curves for speciation of arsenic acid depending on the pH level.

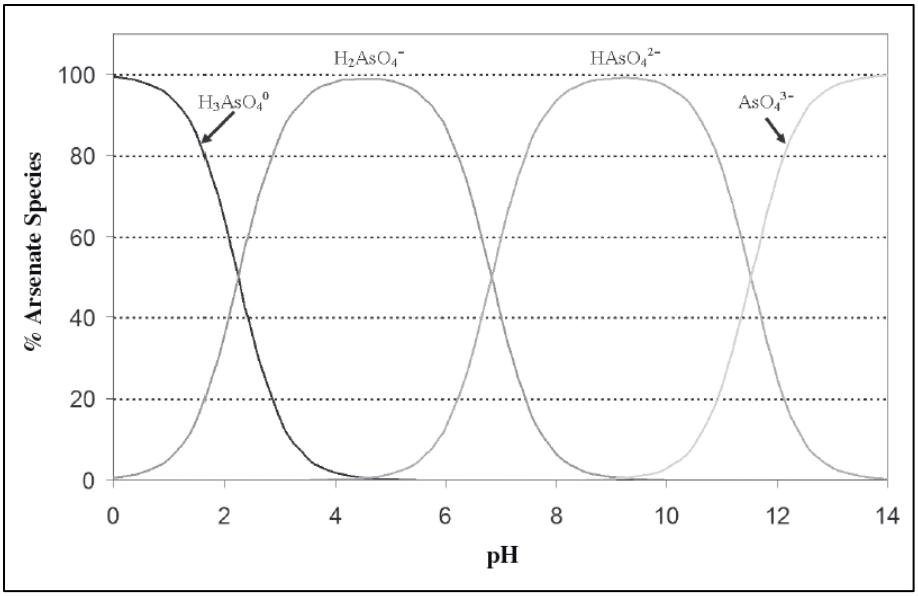


**Figure 1.1** Speciation of arsenic acid with pH. [10]

For removal of Arsenic, Adsorption or sorption is one of the most widely used methods. Iron, aluminum, and manganese oxides widely occur as sorbents and coatings on other solid materials in nature. And these are often considered as important adsorbents for the case of

removing arsenic from water. Below the ZPCs of the oxides, the presence of abundant $\equiv OH_2^+$ is responsible for the net positive charges. The pH of a solution associated with an absorbent effect both the surface charges and the charges of the dissolved arsenic species, which controls arsenic adsorption. [11-12] $H_3AsO_3^0$ adsorbs onto negatively charged surfaces near pH neutral conditions. But, the adsorption of $H_3AsO3^0$ is not as effective as the adsorption of As (V) oxyanions onto positively charged sorbent surface, which is important for the natural adsorption and water treatment. [10]

The oxidation of arsenic refers to increasing valence state as high as +5 through chemical reactions which causes the arsenic to lose its valence electrons. In the oxidation process such as from As(0) to As(III) and from As(III) to As(V), chemical oxidants receive the electrons from the arsenic atom and are reduced. The oxidation of arsenic in natural waters is considerably enhanced by microorganisms, Fe(III) species, nitrate(NO3-), natural organic matter(NOM), or Mn (III, VI) oxide compounds, even in the absence of $O_2$.[9, 13-14] Oxidation under near neutral pH conditions, inorganic As(III) could then be slowly oxidized to inorganic As(V) by the following reaction

$$2H_3AsO_3^0 + O2 \rightarrow H_2AsO_4^- + HAsO_4^{2-} + 3H^+ \qquad (1.1)$$

Chemical oxidents are necessary for oxidation from As(III) to As(V) because oxidation of arsenic with only oxygen in the water is not efficient and slow.

### 1.1.2 Arsenic Source

Arsenic contamination is a serious problem and mostly happens in the groundwater at various location over the world. Human activity such as mining and arsenic-contaminated

products such as pesticides have induced or exacerbated the contamination globally and locally. [15]

Dissolved arsenic in groundwater primarily exists as inorganic As(V) and As(III). This arsenic speciation is largely controlled by changes in redox potential(Eh) of the solution where the speciation exists. Inorganic As(V) generally dominates in surface waters, but As(III)/As(V) ratio can vary greatly with the presence of chemical absorbents in the natural solution. [16]

More than 100 million people have been at risk from the adverse health effect of drinking detrimental levels of arsenic for prolonged periods. Mostly, Asia countries such as Bangladesh, India, Nepal, Pakistan, mainland China, Taiwan, Cambodia, Vietnam, and Iran show the highest leads of arsenic contamination. Large areas of contamination also occur in the Americas (Chile, Argentina, Mexico, and various parts of the United States).[15-16] The arsenic-contaminated areas over the world are shown in the Figure 1.2.


**Figure 1.2** Map showing significant arsenic contamination problems in the United States [17]

Even though the contamination of Arsenic is found worldwide, the region which received the most attention is the Bengal basin, which covers most of Bangladesh and parts of the Indian states of West Bengal, Assam, and Tripura. It has been estimated that more than 57 million people in Bangladesh are drinking water containing over $10\mu gL^{-1}$ of arsenic. [18]

### 1.1.3 Arsenic Toxicity

Arsenic originally was found in various chemical forms and oxidation states in the earth as the twentieth most abundant element. This element was once used intentional for poisoning by royalty, but mostly has been used as a medical agent, pesticide, a growth promoter in semiconductors and manufacture of glass industries. However, Millions of people worldwide are at risk for the development of cardiovascular disease, diabetes, cancer, and other adverse health effects from drinking arsenic-contaminated groundwater. [10] The largest source of arsenic and other metals is usually in foods such as seafood, rice, mushrooms and poultry. But mostly, arsenic poisoning is caused throguh industrial exposure, from contaminated wine or moonshine, or by malicious administration. Since most arsenic compounds lack color or smell, the presence of arsenic is not immediately obvious in food, water or air, thus presenting a serious human health hazard given the toxic nature of element. [19]

In the majority of cases for being exposed to arsenic are through Respiratory, Gastrointestinal, and Dermal absorption. The extent of arsenic poisoning depends on various factor such as dosage or concentration in the medium, valence state of arsenic, qualitative and quantities interspecies differences. It has been found from the research of arsenic toxicity that

blood levels in acutely toxic and fatal cases would be 1000μgL$^{-1}$ or even greater. [10, 19] Table 1.1 lists the chronic and acute symptoms for arsenic poisoning. [20-21]

**Table 1.1** Chronic and acute effects of being exposed to inorganic arsenic

| Human System | Chronic Effects | Acute Effects |
|---|---|---|
| **Cardiac** | Hypertension, peripheral vascular disease, cardiomyopathy | Cardiomyopathy, hemorrhage, electrocardiographic changes |
| **Hematologic** | Anemia, bone marrow hypoplasia | Hemoglobinuria, bone marrow depression |
| **Hepatic** | Hepatomegaly, Jaundice, cirrhosis, fibrosis, cancer | Fatty infiltration |
| **Gastrointestinal** | Vomiting, diarrhea, weight loss | Nausea, vomiting, diarrhea |
| **Neurologic** | Peripheral neuropathy, paresthesia, cognitive impairment | Peripheral neuropathy, ascending weakness, tremor encephalopathy, coma |
| **Renal** | Nephritis, cancer | Tubular and glomerular damage, oliguria, uremia |
| **Pulmonary** | Cancer | Edema, respiratory failure |
| **Skin** | Hyperkeratosis, hypo-or hyperpigmentation, Mees' lines, cancer | Alopecia |

Chronic and acute effects on human organs from arsenic poisoning occur in the same organ system. For the case of acute poisoning treatments can be by gastric lavage, hemodialysis. The effective remediation for chronic arsenic poisoning has not been developed yet. In the case of the already developed chronic arsenic poisoning, minimizing the risk of reexposure to arsenic is the best way.

For the elimination for both inorganic As (III) and inorganic As (V) in most common laboratory animals, urine is the primary route. Comparison of urinary and fecal elimination in

mice under the same amount of oral and parenteral dose reveals that only 4~8% of the dose is eliminated in feces irrespective of route of intake. [22]

## 1.2 Separation Methods for Arsenic Removal

In numerous contaminated regions, arsenic has occurred in natural materials, wastes, and commercial products. High-arsenic contamination can be caused by industrial activity, farming and naturally occurring phenomena which have affects on soil, sediments, gases, or water. To decrease environmental and human health threats from the arsenic contamination, many countries have recently implemented extensive environmental, health and safety regulations regarding arsenic. Methods for treating arsenic in water can be divided into several broad categories. The categories are listed as follows. [10]

i. Adsorption and Ion exchange treatment (e.g., Activated Alumina, Iron oxide minerals)
ii. Precipitation/Coprecipitation treatment (e.g., Lime(CaO), Iron salts, Aluminum salts)
iii. Membrane treatment (e.g., filtration, reverse osmosis, electrodialysis)
iv. Biological treatment (e.g., living organisms (fungi, bacteria), biological material)
v. Emerging treatment

### 1.2.1 Adsorption and Ion exchange treatment

Adsorption in the water treatment technologies refers to the removal of contaminants by causing them to attach onto the surfaces of solid materials, which are adsorbents or sorbents.

Normally adsorption involves ion exchange. [23] Absorption is the assimilation of a chemical species into the inner side of a solid material and this process may include the migration of the solutes into internal pores. [24]

When choosing proper material for an adsorbent, the material has to be large enough to facilitate permeability and water flow while still providing sufficient surface area for numerous sorption and ion-exchange sites. Other desirable properties for being sorbents and ion-exchange media includes (1) ability to remove large amounts of both As(III) and As(V) fast and effectively ahead of regeneration or disposal, (2) capability of being regenerated, (3) high durability in water, and (4) reasonable cost. [25] In the case of arsenic, sorption onto inorganic solids is more convenient than chemical precipitation/coprecipitation method and costs less than ion-exchange resins or membrane filtration. [26]

For the widely used absorbents and ion-exchange media because of their effectiveness, Iron oxides (Figure 1.3), Manganese oxides, Aluminum oxides, activated carbon, Titanium oxides have been selected for removal of arsenic in water.

Iron oxides (II, III) are very effective in removing arsenic from water. The compound for these oxides might have been synthesized or collected from rocks, soils, or sediments. Amorphous iron oxides generally have higher surface area, which provides more ability of absorption and ion-exchange. [27-29] The ability of ferrihydrite to effectively sorb or ion-exchange arsenic depends on several factors, including the age, surface area and exact composition of the compound. Usually, freshly precipitated ferrihydrites are poorly crystalline and have high surfaced areas, which make them ideal sorbents. Another important factor is pH of the arsenic solution because this pH affects competition between As(III) and As(V) for sorption/ion-exchange sites on ferrihydrites. [11]

**Figure 1.3** Iron Oxide Power [30]

Manganese oxides are also effective absorbents and ion exchange media for removing arsenic ions in the water. Manganese oxides are capable of both oxidizing As(III) in water and absorbing the resulting As(V). Amorphous or poorly crystalline manganese oxide sorbents have higher surface areas and are usually more effective sorbents than crystalline varieties. [5,11]

Aluminum oxides, which share some chemical properties with Fe(III), have been used in the form of activated alumina in water treatment systems. This activated alumina is typically produced by thermally dehydrating aluminum oxide to form amorphous, cubic, and other polymorphs of corundum. However, this activated alumina is usually ineffective in removing As(III) from water and pH must be controlled for absorbing As(V) with activated alumina. [31-32]

### 1.2.2 Precipitation/coprecipitation

In many cases, precipitation and coprecipitation methods are more effective for oxidizing any inorganic As(III) to As(V) before treatment. For achieving optimal performance during this oxidation process, pH adjustment is needed. [33] After this pH adjustment process, chemical agents such as lime(CaO), Iron salts, Aluminum salts and water are added into the system to

form the precipitates. These precipitates exist in the form of colloid and have repulsive surface charges which prevent them from agglomerating and settling. Thus, coagulants such as organic compounds, iron or aluminum salts are added for neutralizing the repulsive surface charges. This will finally lead to agglomeration. [34]

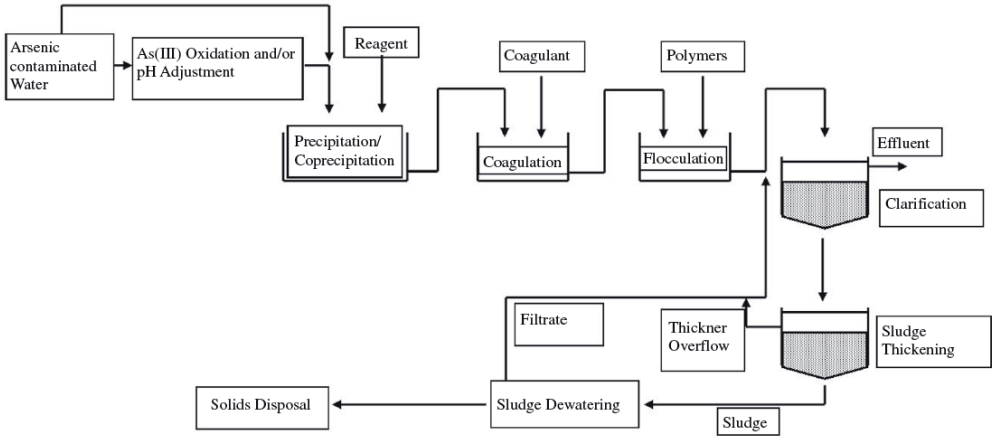


**Figure 1.4** A typical precipitation/coprecipitation system [25]

Lime(CaO) was extensively used for removing As(V) from water through precipitation of calcium arsenates. It was concluded that lime precipitates As(V) from aqueous solutions as hydroxyl and hydrated calcium ($Ca_4(OH)_2(AsO_4)_2 \cdot 4H_2O$, $Ca_5(AsO_4)_3OH$, or $Ca_3(AsO_4)_2 \cdot 3^2/_3H_2O$) rather than anhydrous tricalcium orthoarsenate. [35]

The most popular and effective techniques for removing As(V) from water is iron salts as the chemical agents. Fe(III) chlorides and sulfates(Fe2(SO4)3) react and precipitate iron oxides. Fe(III) salts can coprecipitate about 99% of 0.1-1$mgL^{-1}$ As(V) under pH 7.2. If the arsenic is oxidized before treatment, however, only about 50 to 60% of As(III) can be removed by Iron salts. [36]

Aluminum sulfate($Al_2(SO_4)_3$) and other aluminum salts react with water and precipitate oxides similar to Iron salts. Unfortunately, this aluminum salts type of filtration is not as effective as Fe(III) salts because it has more of a tendency toward being soluble in water than Fe(III) oxide. [37]

### 1.2.3 Membrane treatment

In most cases, filtration method can be used for physical separation of particles, colloids, or other contaminants from water and pressure or vacuum may be applied to filtration systems to cause the removal of contaminants. Pressure filtration makes use of pressure to push the contaminated water through a semipermeable membrane or other type of barrier. Depending on the type of membrane, pH, temperature, pressure, arsenic speciation, or the other characteristics of water, this pressure filtration through membrane can reduce the concentration of arsenic in the water below $10\mu gL^{-1}$. [3,38]

The four major types of pressure filtration processes are microfiltration, ultrafiltration, nanofiltration, and reverse osmosis. Microfiltration is generally used to remove particles with diameters which are greater than about 0.1μm and ultrafiltration can remove the particle diameter size as small as 0.01μm. In the case of nanofiltration, the particle sizes up to 0.001μm could be removed while osmosis can capture particles diameter larger than 0.0001μm.

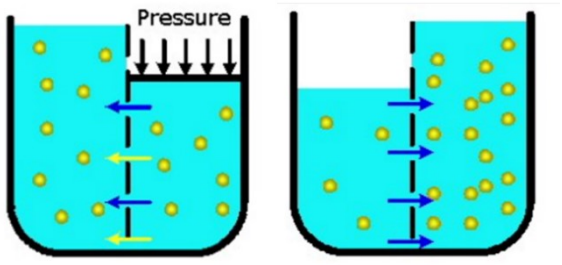


**Figure 1.5** **Left** : Ultrafiltration by pressure **Right** : Reverse Osmosis [39]

In the Figure 1.5, ultrafiltration primarily removes arsenic contaminants by physical sieving and the pores in this system are bigger than arsenic contaminants size. Thus, elecrodialysis can be used for the efficient removal of As(V) by electrically charged membranes such as the example shown in the Figure 1.6. [3]

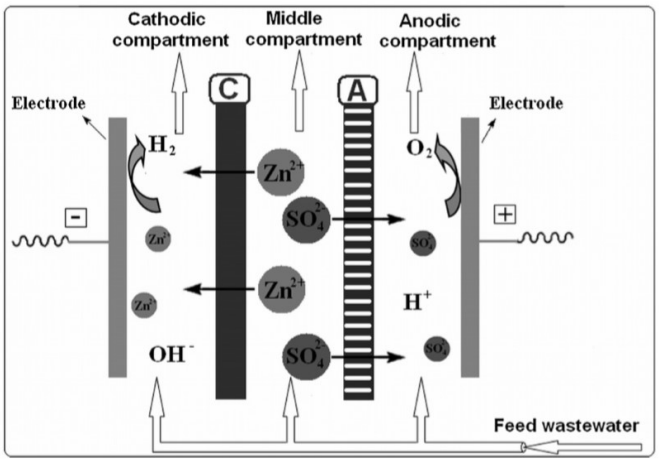


**Figure 1.6** Three-compartment electro dialysis cell and scheme of the ions transport [40]

Reverse osmosis in Figure 1.5, is a suitable technology to reduce As(V) concentration to below 10μgL$^{-1}$. This reverse osmosis membrane contains cellulose acetate, polyamides, polyvinyl alcohol, or other synthetic materials. However, many methods of reverse osmosis cannot always be efficient because of sensitivity to the oxidants, which As(III) can cause by peroxidation process. Some systems operating with bicycle pumps have been developed for removing arsenic from the ground water to be feasible [3]

### 1.2.4 Biological treatment

Biological treatment of contaminated water means using living organisms such as plants, fungi, or bacteria or biological materials to absorb or treat contaminants. It has been attempted to

use human hair, crop wastes, fungal biomass, algae, and chitosan for efficient removal of arsenic from water. Living bacteria, fungi, plants, and other biological organisms have been mentioned for their capability of removing arsenic in the surface water, ground water, soils, sediments, and wastewaters. Also, some bacteria can oxidize As(III) into As(V) and this resulting As(V) can be treated by non-biological methods such as precipitation/coprecipitation or sorption. However, this biological method with fungi and bacteria has to be carefully managed to avoid methylating inorganic arsenic into highly toxic methyl arsine. [41-43]

In some studies, it was shown that arsenic-spiked groundwater can be treated for removing arsenic with *G. ferruginea* and *L. ochracea*. The As(III) level in this groundwater decreased from 200μgL$^{-1}$ to below 10μgL$^{-1}$. And this study also found that bacteria catalytically oxidized the Fe(II) to Fe(III) and As(III) to As(V) . [44]

Another biological treatment used for arsenic removal is phytoremediation, which uses living plants, plants parts, or plant extracts to treat contamination. Growing plants may remove arsenic contaminants in soils, sediments, and water by either absorbing the contaminants on iron coatings or through bioaccumulation within the plant. It has also been found that phytoremediation with living plants may be improved through genetic engineering and understanding of arsenic metabolism and detoxification in plants. [45-47]

Living trees and flowering shrubs may remediate sites through the bioaccumulation of arsenic in their needles, leaves, and other body parts. Pratas et al. (2005) evaluated the accumulation of arsenic in plants at old mine sites in Portugal. It was found that elevated amounts of arsenic were in the old needles of *Pinus pinaster*, *Calluna vulgaris*, and *C. tridentatum* and in leaves from *C. ladanifer*, *Erica umbellate*, and *Quercus ilex* subsp. *ballota*. [48]

### 1.2.5 Emerging Treatment

- **Pyrometallurgical treatment**

Pyrometallurgical treatment makes the usage of heat from incinerators or furnaces to extract or concentrate metals and other inorganic contaminants from soils, sediments, or solid wastes. Pyrometallurgical treatment methods are usually used with solid materials that contain exceptionally high concentrations of inorganic contaminants. Most pyrometallurgical technologies essentially treat contaminated geologic materials and solid wastes as ore deposits. [49] Pyrometallurgical technologies volatilized arsenic from solid materials. The volatilized arsenic is captured by filtration or scrubbing after treating with reductants or fluxing agents. [50-51]

- **Vitrification**

Vitrification means melting of soils, sediments, and solid wastes to primarily incinerate organic contaminants and encapsulate arsenic and other inorganic species into melts. After the melting process, the melted material then cools into an impermeable and chemically resistant glass. For removing arsenic, vitrification method tries to minimize the volatilization of arsenic by incorporating as much of it as possible into slags unlike pyrometallurgical technologies. Especially, arsenic in flue dust or other solid wastes could be stabilized by heating them with lime and air, which leads to less volatile calcium arsenates and arsenates. [49, 52]

- **Electro-kinetic methods**

Electro-kinetic technology refers to removing contaminants from wet soils, sediments, or other solid material by passing them through an electric current zone. These electro-kinetic currents are usually too low to melt the materials unlike vitrification. Kim, Kim and Kim (2005)

estimated the capability of electro-kinetic treatment of arsenic in two fine-grained soils under three-compartment chamber with a platinum anode and titanium cathode on opposite ends. One soil containing a Korean kaolinite was spiked with 1500mgkb$^{-1}$ of As(V). With the additional treatment of $KH_2PO_4$ electrolyte solutions onto the soil, it shows the most effective results for removing arsenic. [53]

## 1.3 Polyethersulfone(PES) Membrane: Overview

Among Ultrafiltration polymer membranes, the most widely used polymer is polyesulfone(PSU) or polyethersulfone(PES) in the Figure 1.7.

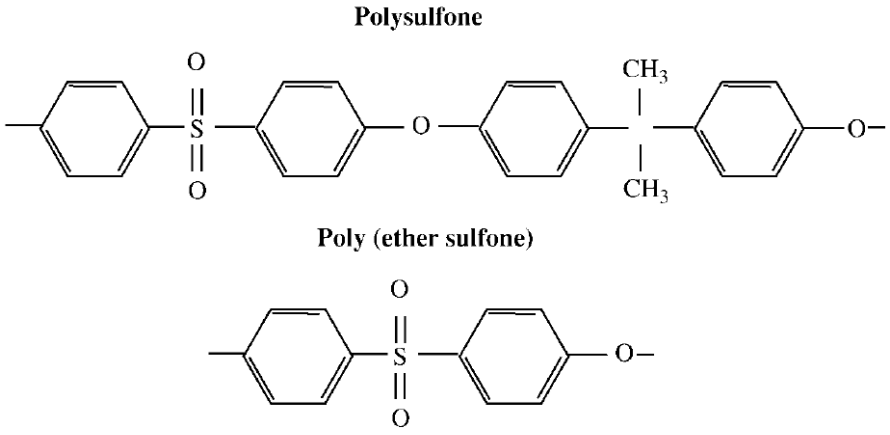


**Figure 1.7** Molecular structure of Polysulfone and Polyethersulfone [54]

The first development of PSU membranes appeared in the 1960s as an alternative to cellulosic membranes. Since then several procedures have been developed and described in the literatures for this Polysulfone membranes [55, 56] and in many cases using the high molecular weight polysulfone Udel P-3500 commercialized by Solvay. The great advantages of PSU in comparison to cellulose acetate is its resistance in extreme pH conditions, as well as its thermal stability. For $T_g$ of PSU, it has 195 and PES case has higher $T_g$ at 230˚C. Both PSU and PES are soluble in chloroform, dimethylformamide and are easily applied in phase-inversion processes. However, this high solubility could be the main drawback of PSU as a membrane material by eliminating the use of polysulfone-supported membranes in the processing of solvent-based feed solution. Another disadvantage of PSU and PES membranes is their hydrophobic character, which prevents consistent wetting in aqueous media. Thus, the membrane should be treated with a hydrophobic agent such as glycerin before drying completely. The other disadvantage

commonly considered is its powerful nonspecific adsorption capacity, which refers to fouling. This fouling finally leads to rapid deterioration of the membrane permeability. [54]

For its thermal stability, PES is one of the most thermally stable aromatic polymers, for which the glass transition temperature, $T_g$, is so high that it can be processed up until 200 ˚C. There has been experiment to measure its thermal stability by methods of thermo-gravimetric analysis (TGA), which checks the point when the thermo-oxidative degradation of PES starts. [57] Data reported previously were measured by using MAT445 type PGC-MS with a Curic point pyrolyzer and OV-1/C545. In the Data, no pyrolyzate was detected at temperature below 385 ˚C. When the pyrolyzate formed at 590 ˚C, it was composed mainly of Sulphur dioxide and phenol. [58,59]

However, the hydrophobic nature of PES makes the membranes prone to be fouled in protein-contacting applications. These are sensitive to many organic solvents, which makes them not suitable to be used as asymmetric support-films for the pervaporation membranes. Even for the applications in aqueous media, the hydrophobic nature of the membrane surface leads to an easy deposition of macromolecular solutes or particles, which have hydrophobic regions. In addition to the fouling due to deposition of large size molecules on the membrane surface, the hydrophobic nature of the materials leads to a poor wetting performance for the pores and low water flux by the filtration process. [61]

This PES, PSU or PPSU(Polyephenysulfone) has been produced by BASF, Solvay, Sumitomo, 3M etc. The slowdown in global economic growth in 2008 and 2009 has impacted on polyarylsulfone (Polysulfone, Polyethersulfone, Polyephenysulfone) sales. The years 2010 and 2011 following the crisis were characterized by significantly above-average growth due to increased application fields for this family of materials such as water and dialysis filters.

Especially, the proportion of polyarylsulfone consumed by the medical sector rose from about 20% in 2010 to the current value of 24%. The consumption of polyarylsulfone as one of High Temperature thermoplastic has increased with its broad range of applications in fields such as aviation, electronics, medical technology, vehicle construction, household and food technology in the Figure 1.8. [60]

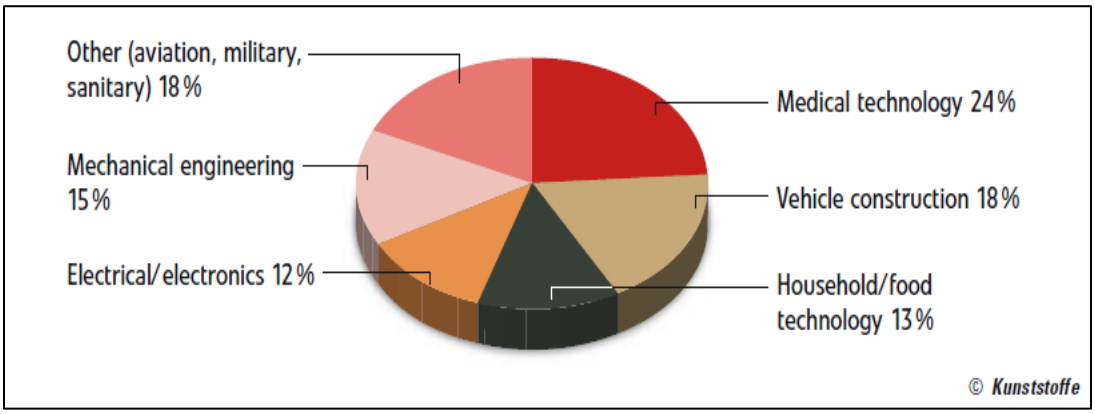


**Figure 1.8** Share of global consumption of polyarylsulfone thermoplastics by application area (2012) [60]

Polymeric materials that lend themselves in particular to water-contact applications will become very important in the short to medium term, as access to clean drinking water becomes critical to the world's growing population. With special processes, it is possible to make Polyethersulfone membranes of which pore number and size can be varied in a wide range. These types of membranes are crucial to water treatment and Polyethersulfone is one of the few polymer materials which make this application feasible. [60]

As a high-temperature engineering thermoplastic, PES should be processed at a higher temperature than when it was originally processed because of its high glass transition

temperature ($T_g$=225˚C). This processing conditions might give rise to different thermal and thermos-oxidation processes that will affect the properties and structure of PES. This thermal processing is more crucial in the case of reprocessing of PES in several cycles. These processing cycles will greatly influence the structure and properties of PES. The selection and control of the processing conditions is, therefore, important in optimizing the structure and properties. [57] Properties of plastics deteriorate mainly as a result of significant changes in polymer structure. In general, the reaction involves a main chain scission, which leads to a decrease in average molecular weight and viscosity of the melted polymers. [62-63] The viscosity of PES rises as a result of repeated processing which leads to the phenomenon known as thickening. The thickening process is a result of a reaction brought about by prolonged shear and heat/oxygen over a specified range of temperature. [57-58]

Synthesized PES membrane by phase inversion method exhibited a typical asymmetric structure composed of a thin skin-layer and a porous bulk with a finger-like structure shown in Figure 1.9 below. [64]

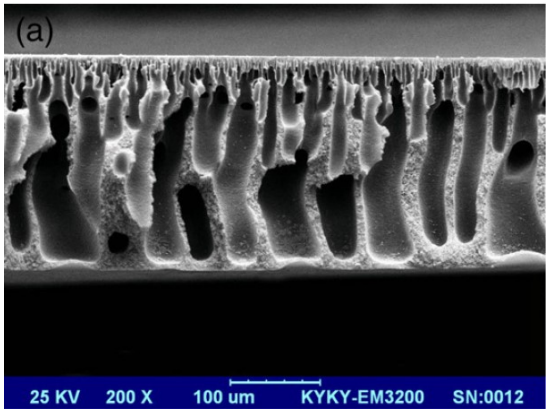


**Figure 1.9** Cross-sectional SEM images of the prepared PES membrane.(Pristine) [64]

Most of the membranes used in industry have an asymmetric structure like as **Figure 1.9**. It consists of two layers: the top one is a very thin dense layer (also called the top skin

layer), and the bottom one is a porous sublayer. This top dense layer governs the performance (permeation properties) of the membrane. In the asymmetric membrane, when the material of the top layer and porous sublayer are the same, the membrane is called an integrally skinned asymmetric membrane. However, if the polymer of the top skin layer is different from the polymer of the porous sublayer, the membrane can be a composite membrane. This composite membrane has advantage over the integrally skinned asymmetric membrane as that it can optimize the performance of the permeation by selecting the top skin layer and sub layer. [65]

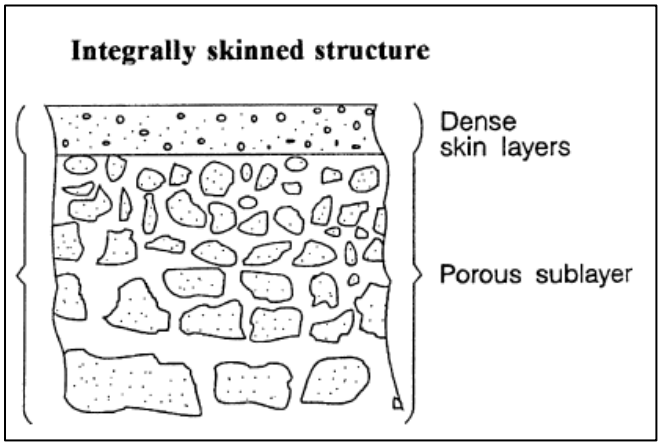


**Figure 1.10** Cross-sectional view of an asymmetric membrane. [65]

## 1.4 Most Relevant Literature Review: Arsenic Removal from Water using Iron Oxide

Ioannis A. Katsoyiannis et al. [66] modified polymeric materials (polystyrene and polyHIPE) by coating their surface with iron oxide and investigated how this modified media can perform for removing inorganic arsenic anions from contaminated water sources. This work has been planned as modified adsorption technology "adsorptive filtration" and is the first research attempt applying polymeric materials as filtration matrices for sorptive filtration of arsenic in the water. For the treatment of polymeric media, Iron hydroxide was coated on the polymeric beads and the filtration of arsenic was conducted.

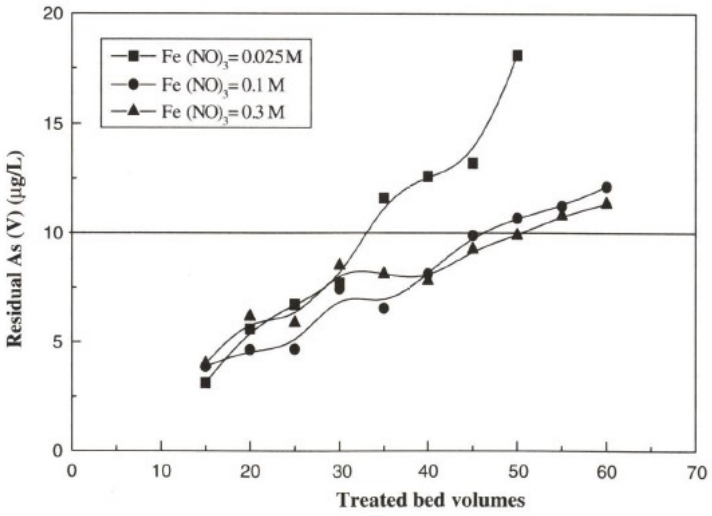


**Figure 1.11** (a) residual arsenic concentration and (b) percentage arsenic removal [66]

**Table 1.2** Iron coated/g polystyrene as affected by the initial concentration of ferric nitrate [66]

| [FE(NO3)] concentration(M) | [Fe] mg Fe/g polystyrene |
|---|---|
| 0.025 | 40 |
| 0.1 | 70 |
| 0.3 | 75 |

The amount of iron hydroxide coated on the surface of polymer beads or media is an important factor when adsorptive filtration techniques are applied. As shown in Figure 1.11 and Table 1.2, with the increase in the amount of iron oxide coated on the surface of filtration media, the adsorption capacity of the media was increased. However, above certain concentration of ferric nitrate which is used for coating iron hydroxide, the amount of coated iron hydroxide did not show any further significant increase in the polymer media. [66]

Qigang Chang et al. [67] investigated performance of removing arsenic by synthesizing iron impregnated granular activated carbon with ferrous chloride. Iron impregnated granular activated carbon(GAC) was stabilized with sodium hydroxide and shown to be very stable at the common pH range in water treatments.

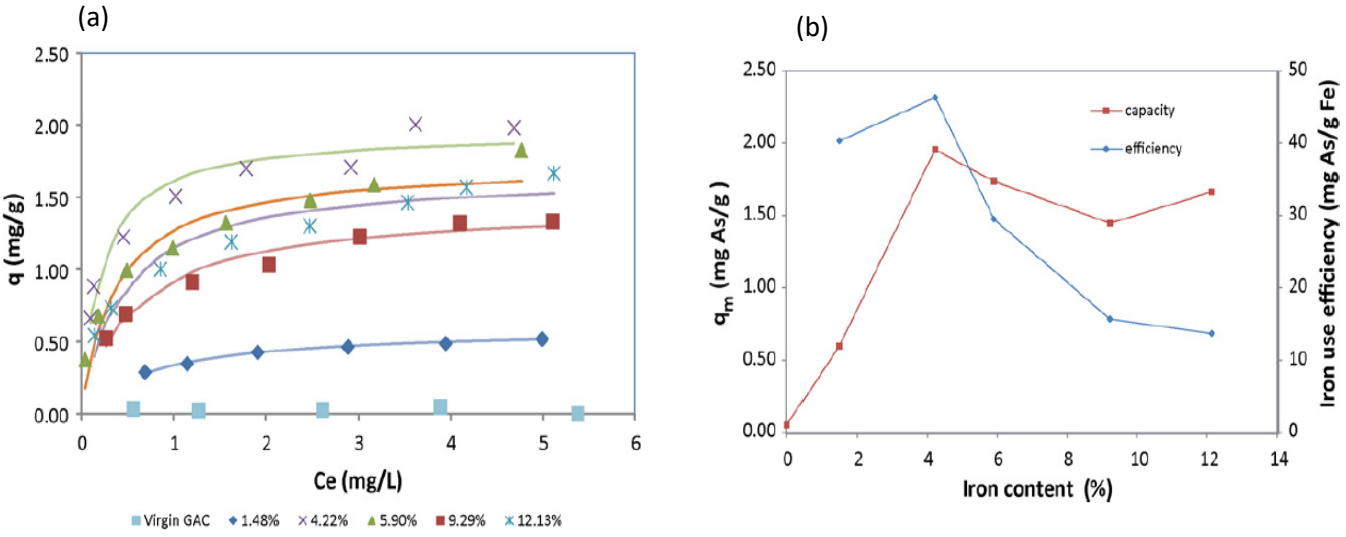


Figure 1.12 (a) Arsenate isotherm curves for Darco 20×50 Fe-GACs (lines are the Langmuir model fits). (b) Relationship between iron content and arsenate adsorption capacity/iron use efficiency. [67]

Arsenate adsorption test from isotherm data were plotted successfully by Langmuir model (Figure 1.12 (a)). The arsenate adsorption capacity by Iron impregnated GACs increased rapidly up to 1.95mg/g when iron concentration increased to 4.22%, while it decreased with more impregnated iron (>4.22%). Further increase in impregnated iron concentration on GACs will resulted in gradual decrease in arsenate adsorption capacity. Impact of the amount of impregnated iron on arsenic adsorption capacity and efficiency were also evaluated and shown as a plot in the Figure 1.12 (b). Iron use efficiency is used to explain the relation between the mass of absorbed arsenate(mg) and a unit mass(g) of impregnated iron. Iron use efficiency maintained at high level from 40mg As/g Fe to 46mg As/g Fe. However, it dropped rapidly to 14mg As/g Fe as iron concentration reaches around 12%. [67]

It was verified from Qigang Chang et al. [67] that as multi-layers and nano-scale iron particles formed, which was observed in SEM analysis, masses of impregnated iron increased faster than the increasing of its surface area. High amounts of iron could cause blockage in PAC porous system, eventually resulting in declining of the surface area for As to be absorbed.

There have been other studies about iron oxide mineral as for removing arsenate depending on its type and pH value and high arsenic removal has been achieved. Figure 1.13 illustrates arsenic (As(III) and As(V)) removal from water in different pH by using different types of iron oxide mineral. [68-71] With hematite as the adsorbent, the maximum As(V) removal reaches around 100% at pH 3-6 like as the Figure 1.13.

Guo, Stuben, and Berner (2007) performed batch and column tests to know the capability of natural hematite for removing arsenic from water. It was investigated by them that the arsenic

removal efficiency increases when the grain size of hematite decreased. It has been found that nitrate ions did not have an influence on the uptake of As(V), while phosphate highly disturbed the adsorption of As(V) into iron oxide. [72]

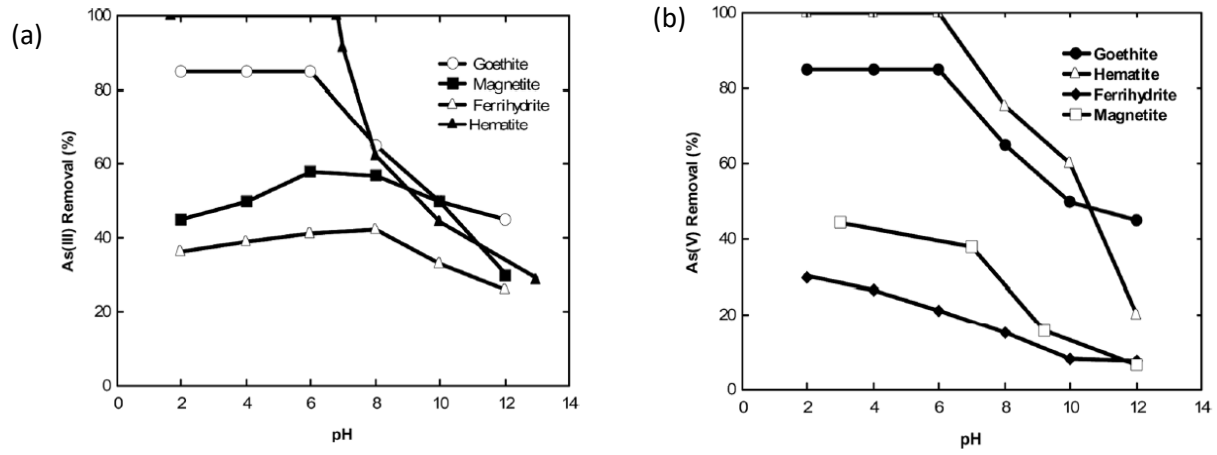


**Figure 1.13** Arsenic removal as a function of pH by adsorption on various iron oxide mineral [68-71]

Narahari Mahanta et al. [73] has investigated the performance of $Fe^{3+}$ immobilized poly (vinyl alcohol) (PVA) nanofibers for removing arsenic from water. For synthesizing PVA/Fe3+ nanofiber, electrospinning technique was used. The adsorption profile of arsenic shows that the maximum value in adsorption experimentation was achieved within 30 min for all concentration ranges as shown in Figure 1.14. Especially for As(III) solution of 20 ppm, the adsorption efficiency value was higher than 95% in 30min and capacity was 20mg/g after 6 hours of extraction. However, in the case of higher arsenic concentration (100ppm) for the same amount of media, the adsorption efficiency is around 90% in 30min and adsorption capacity was recorded as 66mg/g. In the Figure 1.15, the As(V) removal percentage is relatively lower than As(III) removal percentage in the same concentration range when using the same amount of nanofibers. The maximum value of adsorption efficiency was found during the initial 30 minutes

with the adsorption capacity being around 60mg/g at the concentration of 100ppm. In the case of 60ppm solution of As(V), adsorption capacity was extracted as 33mg/g at pH 7.0.

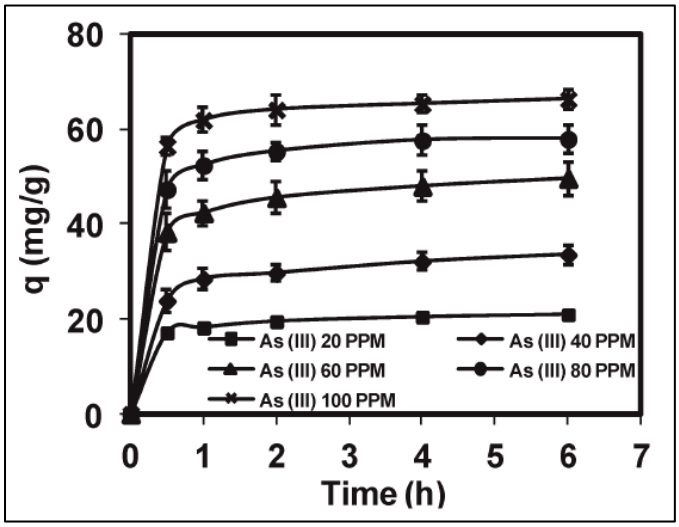


**Figure 1.14** Concentration dependent adsorption kinetics of As(III) ions using Fe3+ incorporated PVA-Fe nanofibers (10mg, pH=7) as a function of time. [73]

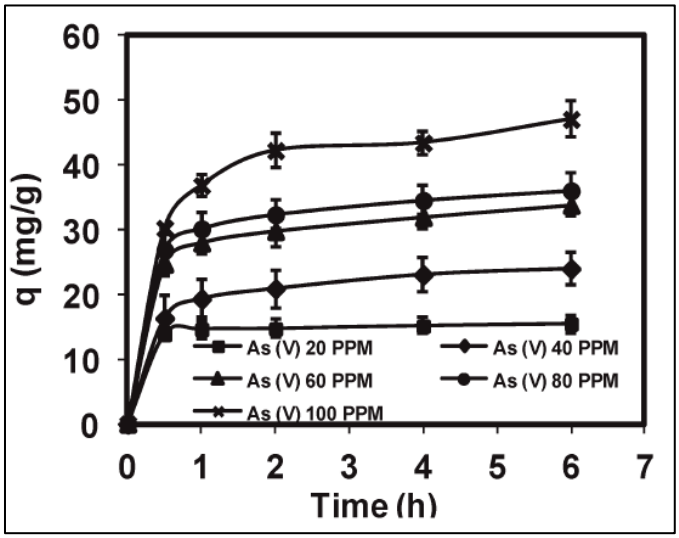


**Figure 1.15** Concentration dependent adsorption kinetics of As(V) ions using Fe3+ incorporated PVA-Fe nanofibers (10mg, pH=7) as a function of time. [73]

It has been verified that adsorption efficiency depends on the surface charge of the absorbent and arsenic anions charge. A mechanism was proposed using spectroscopic data that

shows that arsenate and arsenite ions from bidentate, binuclear complexes with Fe3+ ions. The presences of a free d-orbital on the Fe(III) ion in the PVA/Fe has formation complexes and bridges. [74-76]

## 1.5 Research Objectives

To Study and achieve the performance of PES (Polyethersulfone) composite membrane with modified Iron Oxide nano particles for absorbing Arsenate ion in the solution, the following research objectives were specified in the order of experimentation plan.

**Objective 1**

To improve dispersion of Iron oxide nano particles in the polymer matrix by separating aggregated Nano particles [77], Iron Oxide nano particles' surface were modified by APTES, silane coupling agent. The modification with APTES was characterized by Infrared spectroscopy method. The dispersion of nano particles was analyzed with TGA method.

**Objective 2**

To study the effect of APTES-$Fe_3O_4$ nano particles different wt(%) on the structure and properties of PES(polyethersulfone) composite membrane, FESEM, AFM, contact angle analysis, porosity and pure water flux techniques were utilized.

**Objective 3**

To study the effect of APTES-$Fe_3O_4$ NPs on the performance of adsorption and removal of As(V) ions from water solution, Different solution concentrations (2ppm, 4ppm, 6ppm, 8ppm) were used to develop an equilibrium isotherm model. In the case of kinetic adsorption test, 1ppm solution was utilized under 50psi. All the samples taken for the permeate were analyzed with ICP-MS (Inductively Coupled Plasma) analysis.

# CHAPTER 2

## 2.1 Materials

The raw materials used for the synthesis of PES/APTES-Iron Oxide Nano Particles (A-$Fe_3O_4$-NP) were Polyethersulfone(PES) pellet, Polyvinylpirrolidone(PVP), N, N-Dimethylacetamide (DMAc), Aminopropyltriethoxysilane(APTES), and Iron Oxide Nano Particle. These are purchased from commercial sources and mentioned in each material sections. Other raw materials for As(V) adsorptions were Distilled water and Sodium arsenate dibasic heptahydrate ($Na_2HAsO_4 \cdot 7H_2O$).

### 2.1.1 Polyethersulfone(PES)

PES(Polyethersulfone) are characterized by -$SO_2$- linkages. They are rigid and tough thermoplastics with $T_g$ range of 180-250˚C. Chain rigidity is derived from the relatively immobile and inflexible phenyl sulphone groups, and toughness from the connecting ether oxygen. [78] Its chemical structure is shown in the Figure 2.1.

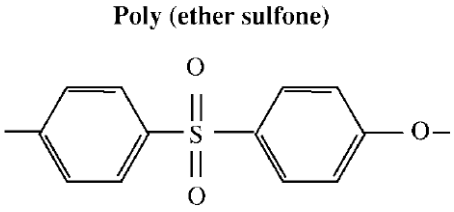


**Figure 2.1** Polyethersulfone chemical structure [54]

PES(Polyethersulfone) has excellent high temperature properties and chemical inertness. It can be used continuously in the temperature range of 150-200˚C. For a wide variety of applications requiring sterilization and cleaning at high temperature, its ability to maintain its

mechanical properties in wet, hot environments is considered a key point in industrial use. The PS family has wide pH tolerance from 1 to 13, which contributes to its usages for the cleaning purposes. PES can also be easily fabricated into many complex configurations and modules by injecting its resin into a mold.

However, PES has limitations for the industrial filtration application with low pressure limits and strong hydrophobicity. It is prone to interact with many kinds of solutes in the aqueous system thus it has more fouling phenomena than hydrophilic polymers like cellulose. [78] There have been a lot of efforts within the research and manufacturing field for overcoming this fouling phenomena by adding fillings such as metal oxide Nano particles or Nano Clay for the increase of hydrophilicity of PES.

In my research project, PES Ultrason E6020P has been purchased from BASF Company(Germany) with the specification of Molecular weight, 58,000g/mol as the base polymer, PES(Polyethersulfone). 18 wt% of PES pellets were dissolved in DMAc(Dimethylacetamide) solvent in a water bath and placed under reflux condenser system for 24hrs at 50˚C to make PES pellets melted into the solvent homogenously for the next Nanoparticle mixing steps.

### 2.1.2 Polyvinylpirrolidone (PVP)

For the purpose of high performance of filtration from the membrane, especially UF membranes, decent porous structure has to exist in the polymer membranes. To achieve this purpose, Polyvinylpirrolidone(PVP) have been widely studied and used for being added into PES polymer resin with its high contribution of effective surface pore structure after PES casting.

With the interaction of O=C-N< function groups in the PVP in the Figure 2.2 and O=S=O group, most active polar functional groups in PES, PVP become entrapped in the PES network and form an integral part of the polymer structures, providing not a only swelling effect but also a hydrophilic nature to the polymer.

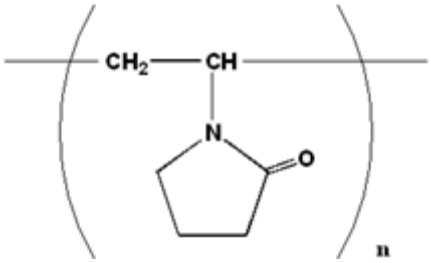


**Figure 2.2** Chemical Structure of Polyvinylpirrolidone(PVP) [79]

The solution structure formed under interaction forces between PVP and PES causes an increase in the size of the largest pores involved in the pore size distribution and consequently increases the permeation rate. [80] Thus, it has been concluded that the primary effect of PVP in the PES casting solution is on the structure of casting solution and, as consequence, on the pore size and the pore size distribution of the membrane. [80]

In this research project, PVP was purchased from Sigma Aldrich with the specification of average molecular weight, 29,000 and 1wt% of PVP was added in the PES casting solution for forming the porous structure in membrane.

### 2.1.3 N, N-dimetylacetamide (DMAc)

In the preparation of membrane process, diffusion induced phase separation was employed, the exchange of solvent and non-solvent between polymer solution and coagulation bath played an important role. N, N-dimethylacetamide (DMAc) was chosen as the solvent in this research based on the past research working on the polymer membrane formation

mechanisms with different solvents. Among several solvent candidates for PES, such as N, N-dimetylacetiamide(DMAc), N, N-dimethylformamide (DMF), 1-methyl-2-pyrrolidone (NMP), the casting solutions including DMAc as its solvent for dissolving PES pellet showed the best performance for forming a highly porous structure in membrane. [81] As the membrane performance is a function of membrane structure for higher filtration flux, DMAc was selected as the solvent for dissolving PES pellets and forming the PES membrane in coagulation bath.

N, N – Dimethylacetamide (DMAc) is a colorless, high boiling, polar, hygroscopic liquid. DMAc is a good solvent for a wide range of organic and inorganic compounds and its polar nature shown in Figure 2.3 enables them to combine to solvents for high yield of the final products. [82]

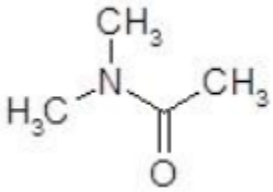


**Figure 2.3** Chemical Structure of N, N- Dimethylacetamide (DMAc) [82]

In this research project, N, N – Dimethylacetamide (DMAc) were purchased from Sigma Aldrich with the specification of 99% purity. Weight percent of DMAc in each PES/APTES-$Fe_3O_4$ sample was variant as 81%, 80%, 79% and 78% depending on the weight percentage of APTES-$Fe_3O_4$ (0%, 1%, 2%, 3%).

### 2.1.4 Iron Oxide Nano Particles ($Fe_3O_4$-NP)

Iron Oxide Nano Particles($Fe_3O_4$-NP), purchased from Sigma Aldrich(USA) and added to PES after modification with APTES(Aminopropyltriethoxysilane), have the nano size range of 50-100nm. As the chemical formula, Fe3O4, it has the following physical properties: Spherical Magnetite nano powder, 97% trace metals basis, molecular weight 231.53g/mol, BET surface area over 60$m^2$/g, dark black color, melting point 1538 ˚C, and bulk density 0.84 g/mL. [83]

The magnetite($Fe_3O_4$) nano particles with their multifunctional properties such as super paramagnetism, low toxicity, excellent thermal properties, good biocompatibility and biodegradation, have been widely used for biotechnology and biomedical applications. [84] Also, magnetic particles assist in effective separation of catalysts, nuclear waste, biochemical products and cells. [85-87] Magnetically driven separations with Iron Oxide nano particles happens efficiently with the combination of high dispersion of small and magnetically separable catalysts and reactivity with separation system. [84]

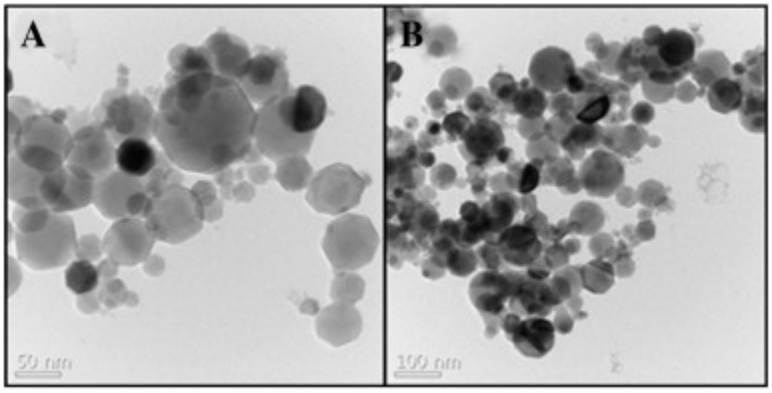


**Figure 2.4** FE-TEM images of the iron oxide nanoparticles (Magnetite and maghemite) (A) Scale bar: 50nm. (B) Scale bar: 100nm. [88]

Magnetic properties of Iron Oxide Nano Particles has been extended to include environmental remediation of toxic elements because it can be separated easily with magnet. The

removal of As(V) from drinking water has been targeted in this research study by considering its magnetic separation ability based on the previous literature review.

The Iron oxide weight percentage for each PES (Polyethersulfone) differs as written below in the table.

**Table 2.1 Weight Concentration of chemical components in each PES sample**

| Wt(%) | PES | APTES-$Fe_3O_4$ | DMAc | PVP |
|---|---|---|---|---|
| M1 | 18 | 0 | 81 | 1 |
| M2 | 18 | 1 | 80 | 1 |
| M3 | 18 | 2 | 79 | 1 |
| M4 | 18 | 3 | 78 | 1 |

### 2.1.5 Aminopropyltriethoxysilane(APTES)

For forming good quality of Polyethersulfone membrane with well dispersed Iron Oxide Nano Particles, Iron Oxide particles were chemically modified with APTES, silane agents. The main difficulties with polymer nanocomposites is the prevention of particle aggregations caused by specific surface area and volume effects. The modification with APTES improves the interfacial interactions between the inorganic particles (Iron Oxide) and polymer matrix(PES). This particle surface modification generates a strong repulsion between nanoparticles. [77]

APTES(3-aminopropyltriethoxysilane) is the most commonly used aminosilane and its popularity is contributed to complexities in usages. First, APTES in the Figure 2.5 has many possible ways to interact with surface silanol/silanolate groups by hydrogen bonds, electrostatic attractions, and siloxane bonds. Secondly, it has three ethoxy groups per molecule and is capable of polymerizing in the presence of water, which leads to many possible surface structures such as

covalent attachment, two-dimensional self-assembly (horizontal polymerization), and multilayers (vertical polymerization). Thirdly, excess water results in not only uncontrolled polymerization of silane molecules on surface, but also formation of oligomers and polymers of silanes in bulks, which can also interact and attach to the surface. [89]

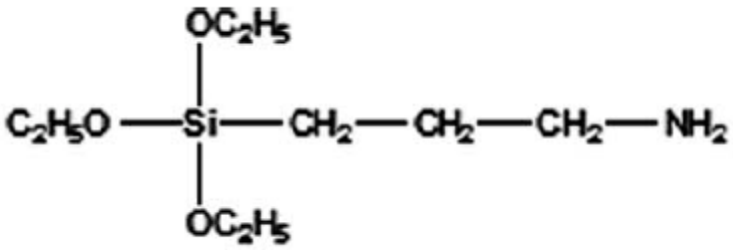


**Figure 2.5** Chemical Structure of Aminopropyltriethoxylsilane [91]

Thus, APTES(3-aminopropyltriethoxylsilane) compound has been considered as an important silane coupling agent and widely used grafting agent to promote interfacial behavior of inorganic oxides including silica, ceramics, titania, and magnetic iron oxide Nano particles. [90]

In this research project for the surface modification of Iron Oxide Nano Particles, APTES was purchased from Sigma Aldrich with its specification of purity, 98.5% and molecular weight, 221.37g/mol.

## 2.2 Synthesis and Characterization

### 2.2.1 Synthesis of PES Nanocomposite Membrane

The experimentation steps for synthesizing Polyethersulfone(PES) membrane impregnated with APTES-$Fe_3O_4$-NP were developed based on the reference studying PES with differently modified $Fe_3O_4$-NP for absorbing copper ion through filtration. [92] For dissolving PES in

DMAc, round bottom flask filled with DMAc, PES was placed in water bath at 50˚C and stirred with a magnetic stirrer for 24 hours under a condenser reflux setup as described in the Figure 2.6.

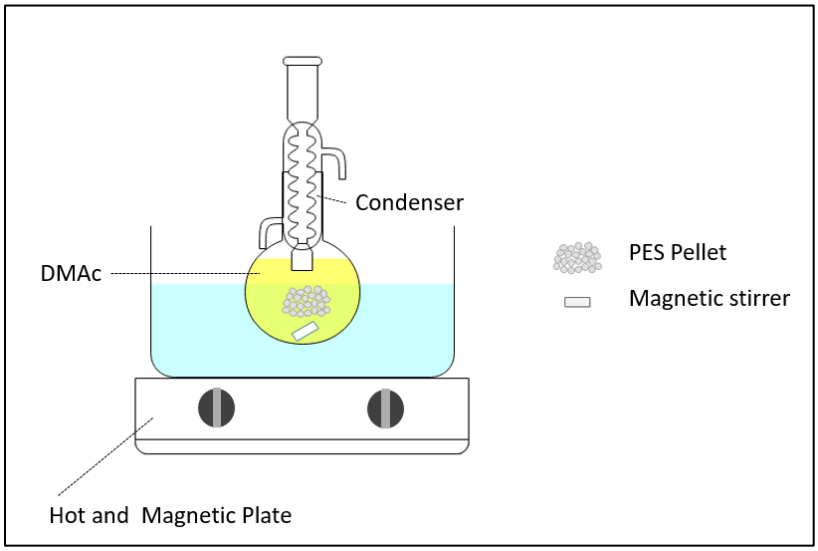


**Figure 2.6** Experimental setup for dissolving PES pellet in DMAc

For the mixing magnetic Nano Powder, APTES-$Fe_3O_4$ into PES resin after dissolving into 30 wt.% of total DMAc, modified $Fe_3O_4$-NPs were mechanically dispersed in DMAc by ultrasonication, Probe type (20% Amplitude, 1 pulse) for 30 minutes. Then, Fe3O4-NPs in DMAc were added into PES resin and this solution was mechanically mixed for 2 hours at 3500rpm for homogenous dispersion of $Fe_3O_4$-NPs. To achieve better mixing after mechanical mixing process, this PES-APTES-$Fe_3O_4$ solution were mixed with an Acoustic mixer for 45 minutes at 40% Intensity and with probe type ultrasonicator (60% Amplitude, 2 pulse) for 2 minutes.

After completing the homogenous mixing steps, the PES-APTES-$Fe_3O_4$ solution was casted on a glass plate in Distilled Water with Doctor Blade (number 8, 200µm) at room

temperature. Each casted membrane was solidified in DI water for 24 hours and dried in a vacuum oven for 24hours. Each composition weight percent is described in Table 2.1.

### 2.2.2 Synthesis of $Fe_3O_4$-NP grafted with APTES

For modification of $Fe_3O_4$-NPs surfaces, 2g of $Fe_3O_4$-NPs were treated each time in pure ethanol 100mL with 2wt% of APTES of this solvent. The experimentation development was based on the reference studying for kinetics of APTES Silanization of Iron oxide Nano particles. [90]. Pure ethanol solvent(98%) 100mL plus 2g of $Fe_3O_4$-NPs was placed into three neck round bottom flask (250mL) and mixed with a mechanical mixer at 4000rpm. Nitrogen was supplied into this flask until 2mL of APTES was added into system with syringe then all the neck of the flasks were blocked with a rubber cap for 2 hours mixing at 65˚C.

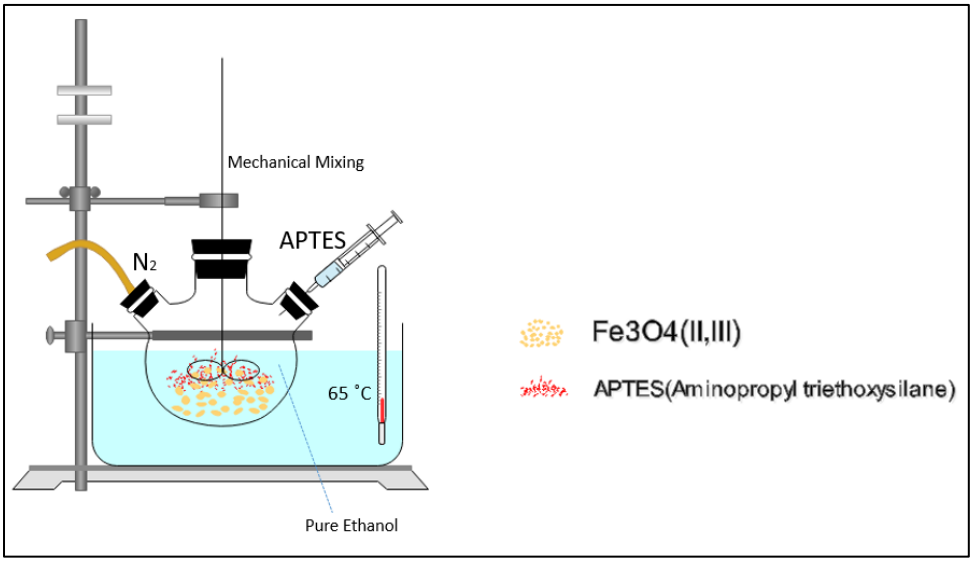


**Figure 2.7** Experimental setup for modification of Fe3O4-NPs with APTES

After finishing treatment, the APTES-$Fe_3O_4$-NPs were washed with anhydrous ethanol 4 times by distillation with magnet. The treated NPs were then dried in a vacuum oven for 24hrs.

For this modification, the reference [90] studied the modification mechanism by 3 steps, hydrolysis of APTES, surface attachments and condensations described in Figure 2.8.

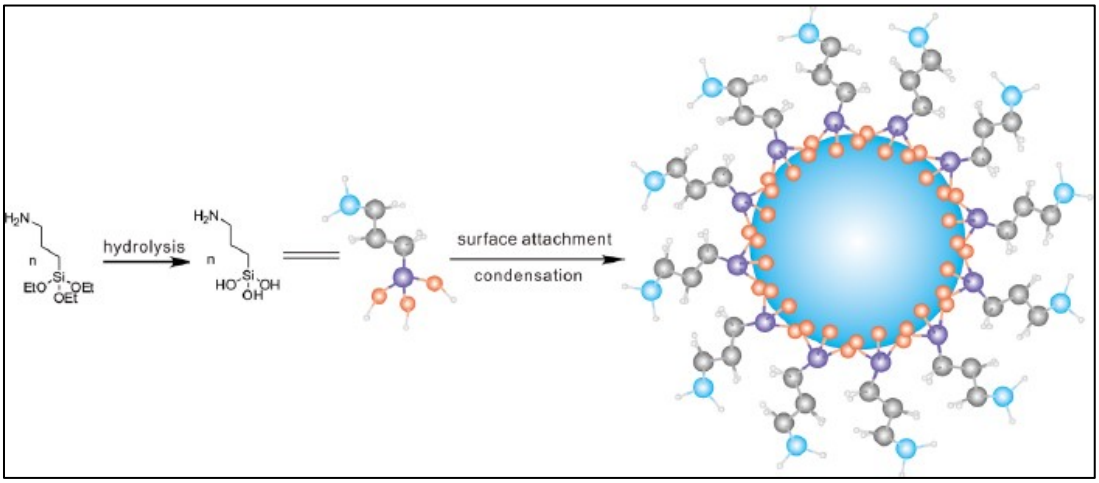


**Figure 2.8** Silanization of magnetic iron oxide nanoparticles with APTES [90]

The treatment condition of NPs with APTES was referred from the study [93] for effect of APTES-NPs on PES performance. (65˚C in oil bath, 2hr)

### 2.2.3 Characterization of $Fe_3O_4$-NP grafted with APTES

2.2.3.1 IR

Iron Oxide Nano Particles ($Fe_3O_4$-NP) treated with APTES were characterized with Infrared Spectroscopy(IR) Tracer 100 (Shimadzu) by comparison with non-treated $Fe_3O_4$-NP.

From the APTES-$Fe_3O_4$-NPs, the modified functional group were expected for - $CH_2$, - $CH_3$ (wavelength: 2,840–2,960 $cm^{-1}$), -$NH_2$ (wavelength: 1560$cm^{-1}$) based on APTES chemical structure and mechanism of its modification. [90], [91] The IR spectrometer scanning was carried out in the range of 5000$cm^{-1}$ to 350$cm^{-1}$ with the transmission intensity mode, Happ-Genzel Apodization, 200 times of scan, 4$cm^{-1}$ resolution.

2.2.3.2 TEM

To characterize the modification of $Fe_3O_4$-NPs, Transmission electron microscopy (TEM, Hitachi H-9000NAR microscope) with an attached Noran Energy Dispersive Spectrometer was operated at 300keV. For the sample preparation, small amount of powder transferred by wood pick to agate mortar and a few drops of ethanol were added. Agate pestle used to gently break up aggregates. Plastic pipette used to disperse nanoparticles on Lacey Carbon copper mesh TEM grid. Sample dried at room temperature in air.

### 2.2.4 Characterization of PES Nanocomposite Membrane

2.2.4.1 FESEM

Field emission scanning electron microscopy (FESEM, Hitachi S-4800, Japan) was used to analyze morphology of the membrane and agglomerated APTES-$Fe_3O_4$-NPs. For taking the image of each membrane sample (M1, M2, M3, M4), FESEM was operated with the condition of 1000 times magnification, 8mm depth, 7.6 kV . The membrane cross section was created by being cut after Cryo-snap method(Freeze-Fracture) in liquid nitrogen. [94] The membrane samples on the stage support were coated with the 5nm thickness of Ir.

2.2.4.2 TGA

Thermogravimetric Analyzer (TGA, SDT 2960) was carried out in the range of 30-1000˚C under air atmosphere with a flow of 50mL/min, heating rate of 20˚C/min and sample

mass around 16mg. TGA analysis were conducted on 3 times on different locations of each sample. (M2, M3, M4)

#### 2.2.4.3 AFM

Atomic force microscopy was employed to analyze the surface morphology and roughness of the membrane samples. The Atomic Force Microscope apparatus used was the Agilent 5420 made in the USA. 1cm width and 2cm length size of membranes were prepared for each sample and taped into the glass slide by dual side carbon tape. 2μm×2μm were scanned with tapping mode, the speed of 1.2 In/s and 256×256 resolution. The surface roughness parameters of the membranes are expressed in terms of the mean roughness($S_a$), the root mean square of the Z data($S_q$) and the mean difference between the highest peaks and lowest valleys($S_z$) through the software, Picoview 1.14. 2D and 3D roughness images with scanning data were processed through open source program, Gwyddion 2.51.

#### 2.2.4.4 Contact Analysis

The hydrophilicity of membranes was evaluated by measuring the contact angle between water droplet and membrane surface by using a contact angle goniometer (Rame –Hart Goniometer). The results were the average of five tests at random spots on each membrane surface.

2.2.4.5 Porosity and mean pore size

Overall porosity ε of the prepared nanocomposite membranes was calculated by the gravimetric method using the following equation [95]

$$\varepsilon = \frac{\omega_1 - \omega_2}{A \cdot l \cdot d_w} \quad (1)$$

where $\omega_1$ and $\omega_2$ are the weight of the wet and dry membranes, A is the membrane area ($m^2$), $l$ is the membrane thickness(m), and $d_w$ is the water density (0.998g/$cm^2$). The membrane thicknesses were measured with a Digimatic Digital Thickness Gage (Mitutoyo 547-400S, range: 0 – 0.47 inch) 20 times per every membrane sample and the average values were used.

Moreover, the membrane mean pore radius ($r_m$) was determined by Equation (2) (Guerout-Elford-Ferry equation):

$$r_m = \sqrt{\frac{(2.9 - 1.75\varepsilon) \times 8\eta l Q}{\varepsilon A \Delta P}} \quad (2)$$

Where Q is the volume of the permeated pure water per unit time ($m^3/s$), η is the water viscosity ($8.9\times10^{-4}$ Pa s) and ΔP is the applied pressure (0.345 MPa). [95, 96]

2.2.4.6 IR Analysis

Infrared Spectroscopy(IR) Tracer 100 (Shimadzu) was used for characterization of pristine PES and PES-A-$Fe_3O_4$-NPs (1wt%) membrane. Between pristine PES and PES-A-Fe3O4-NPs, Hydroxyl functional group (H-O-H), Fe-O functional group was expected for the derivation. Each membrane sample was analyzed in the wavelength range of 5000$cm^{-1}$ to 350$cm^{-}$

$^{1}$ with the transmission intensity mode, Happ-Genzel Apodization, 100 times of scan, and 8$cm^{-1}$ resolution.

### 2.3 Membrane Filtration and Adsorption Experiments

#### 2.3.1 Pure Water Permeability(PWP)

The prepared membrane with different A-$Fe_3O_4$-NPs concentrations were cut into a circular shape for fitting into the bottom of the membrane cell (50 ml Amicon Stirred Cell, Millipore, Area: 13.4$cm^2$). The membranes were initially soaked with distilled water for 30 minutes and stabilized under distilled water by Nitrogen pressure at 50psi for 30 minutes. The permeate flux was calculated using the following equation.

$$\mathrm{PWP} = \frac{Q}{A\ t\ \Delta P} \tag{3}$$

Where Q is the permeate volume(L), A is the membrane area($m^2$), t is the time(h), and ΔP is the pressure difference across the membrane sides. The differential pressure used was 50psi during 30 minutes for each membrane.

#### 2.3.2 Experimental Sep up for Dynamic adsorption and Arsenate Rejection (%R).

The Experimental sep up is composed of 50mL Amicon Stirred Cell (EMD Millipore, Billerica, MA, USA). 1ppm of Sodium arsenate dibasic heptahydrate was placed into 1000mL for making the working solution. After Arsenate solution was forced to pass through the

membrane by nitrogen pressure at 50psi, both the As(V) feed and permeate composition were evaluated by Inductively Coupled Plasma(ICP) analysis (ICP-MS-2030, Shimazu, Japan).

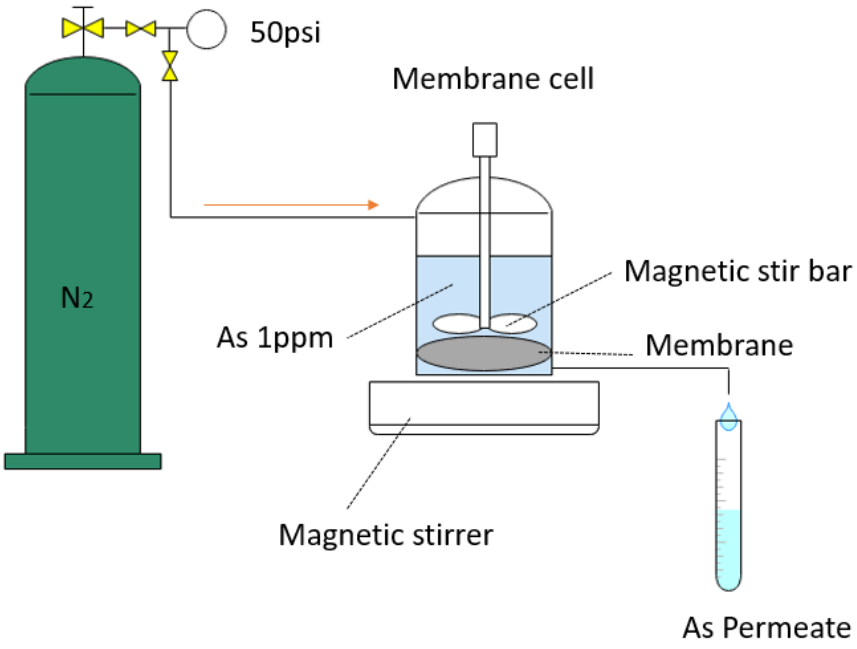


**Figure 2.9** Experimental Sep-up used for Arsenate (As) removal from solutions.

Both feed and permeate samples were stabilized with nitric acid (2%v/v $HNO_3$) before ICP-MS analysis.

The percentage of Arsenic removal %R was defined and calculated as follows:

$$\%R = \frac{((C_0 - C_t) \times 100)}{C_0} \quad (4)$$

where $C_0$ is the initial As concentration and $C_t$ is the As content at specific time t.

### 2.3.3 Batch adsorption analysis

The adsorption behaviors of As(V) with the different PES-A-$Fe_3O_4$ membrane samples were studied with batch experimentation. All adsorption isotherm experiments were conducted in a series of sealed volumetric flask containing 0.05g of each membrane sample and 100mL of As(V) solution in 4 different concentration. (2ppm, 4ppm, 6ppm, 8ppm). The solution containing each membrane sample was stirred with magnetic stir bar for 24 hours at 25 ˚C at 200 rpm. Arsenate was absorbed into each of the membrane samples and reached equilibrium concentration after 24 hours. The concentration of As(V) residual was measured with Inductively Coupled Plasma(ICP) analysis (ICP-MS-2030, Shimazu, Japan). Experimental Set-up is descried in the Figure 2.9.

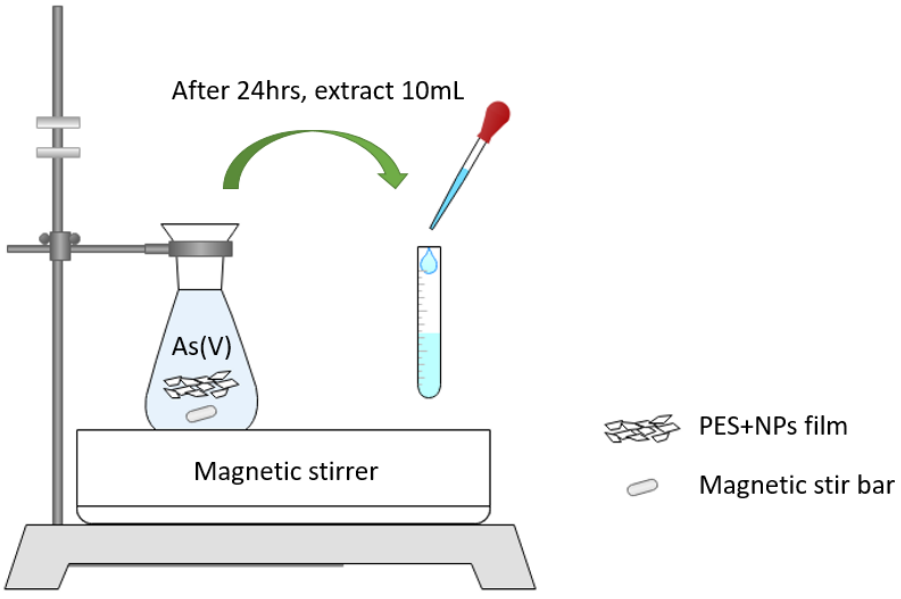


**Figure 2.10** Experimental Set-up for Batch adsorption tests

The equilibrium adsorption amount and removal efficiency of As(V) by the membranes were calculated as follows:

$$q_e = \frac{((C_0 - C_e) \times V)}{M_m} \quad (5)$$

where $C_0$ (mg/L)is the initial As concentration and $C_e$ (mg/L) is the As content at equilibrium. V is the total volume(L) of the arsenate solution(0.1L) and $M_m$ is the mass(g) of dry membrane used in the adsorption study.

### 2.3.4 Inductively Coupled Plasma(ICP) analysis

Inductively Coupled Plasma Mass Spectrometry of ICP-MS is an analytical technique used for elemental determinations. ICP-MS has many advantages over other elemental analysis techniques such as atomic absorption and optical emission spectrometry, including ICP atomic Emission Spectroscopy. [97]

An ICP-MS combines a high temperature inductively Coupled plasma source with a mass spectrometer. The ICP source then converts the atoms of the target elements in the sample into ions. These ions are then separated and detected by the mass spectrometer. Figure 2.10 shows the schematic drawing of an ICP source. [97]

For the Mass spectrometry technique, three essential parts of the instrumentation could be identified: (i) the ion source, in which the ions are provided, (ii) the mass spectrometer itself, in which the ions are separated from one another as a function of their mass-to-charge ratio, and (iii) the detection system that converts the ion beam into a measurable electrical signal. [99]

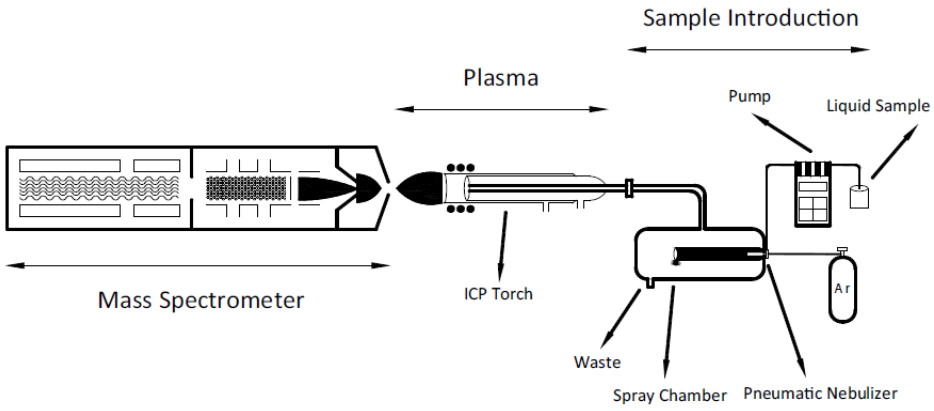


**Figure 2.11** Schematic representation of the essential parts of mass spectrometric instrumentation [98]

To summarize, Table 2.2 below is a list of the characterization experiments and the purpose of each

**Table 2.2 List of characterizations and purpose of each**

| Characterization | Purpose |
|---|---|
| FESEM | To analyze morphology of membrane and A-$Fe_3O_4$ NPs for the change of pore structure in cross-section |
| TGA | To evaluate the degree of dispersion of A-$Fe_3O_4$ NPs in PES membrane |
| AFM | To measure roughness value of prepared membrane |
| Contact Angle Analysis | To evaluate hydrophilicity of prepared each membrane |
| Porosity and mean pore size | To verify the effect of A-$Fe_3O_4$ NPs on the pore size and percentage of porous structure |
| IR analysis | To confirm the surface modification of $Fe_3O_4$ NPs |
| Pure water flux | To confirm the degree of porosity |
| Batch adsorption analysis | To define the relation between equilibrium adsorption capacity of prepared membranes vs initial concentration of As(V) solution |
| Dynamic adsorption analysis | To study the kinetic adsorption phenomena As(V) of prepared membranes under pressure through membrane cell |
| ICP Analysis | To analyze the As ion concentration in each permeate samples |

# CHAPTER3

# RESULTS AND DISCUSSION

## 3.1 Characterization Analysis

### 3.1.1 FESEM Analysis

Cross-section FESEM image of PES-A-$Fe_3O_4$ membrane and pristine PES membrane are displayed in Figure 3.1 to evaluate the change in porous structure. Each membrane exhibited an asymmetric structure composed of a skin-layer and porous bulk containing finger-like channels. It has been shown that there is significant difference in skin layers' thickness and porous bulks by adding APTES-$Fe_3O_4$.

In the Figure 3.1 (c) and (d), it is verified that addition of APTES-$Fe_3O_4$ NPs contributes into making a more porous structure in the top layer due to an increase in the solution thermodynamic instability of the non-solvent system. This thermodynamic instability caused rapid mass transfer between solvent and non-solvent components in the solidification process and then this phenomenon leads to a larger porous structure in membrane skin layers. [95]

However, adding more APTES-$Fe_3O_4$ NPs decreased the porous radius in the skin layer because of increased viscosity of the casting solution and agglomeration of NPs with a higher weight percent of NPs. High viscosity typically delays the mass transfer process between non-solvent and solvent, which finally contributes to the formation of the smaller pores in the skin top layers. [95]

For the bulk layers in the cross section, addition of APTES-$Fe_3O_4$ affects the porosity and pore shape Figure 3.1. According to FESEM, sub-layer micro-voids have been formed with a

higher concentration of APTES-$Fe_3O_4$ and the largest pore sublayer pore structure were found in the PES-A-$Fe_3O_4$ 2wt% and PES-A-$Fe_3O_4$ 3wt%. These micro voids sizes' extension across the membrane was induced by increased miscibility of non-solvent with hydrophilic $Fe_3O_4$ NPs. Growth of micro-voids in sub-layer by addition of metal oxides nanoparticles to membrane has been proven in the past. [95, 100]

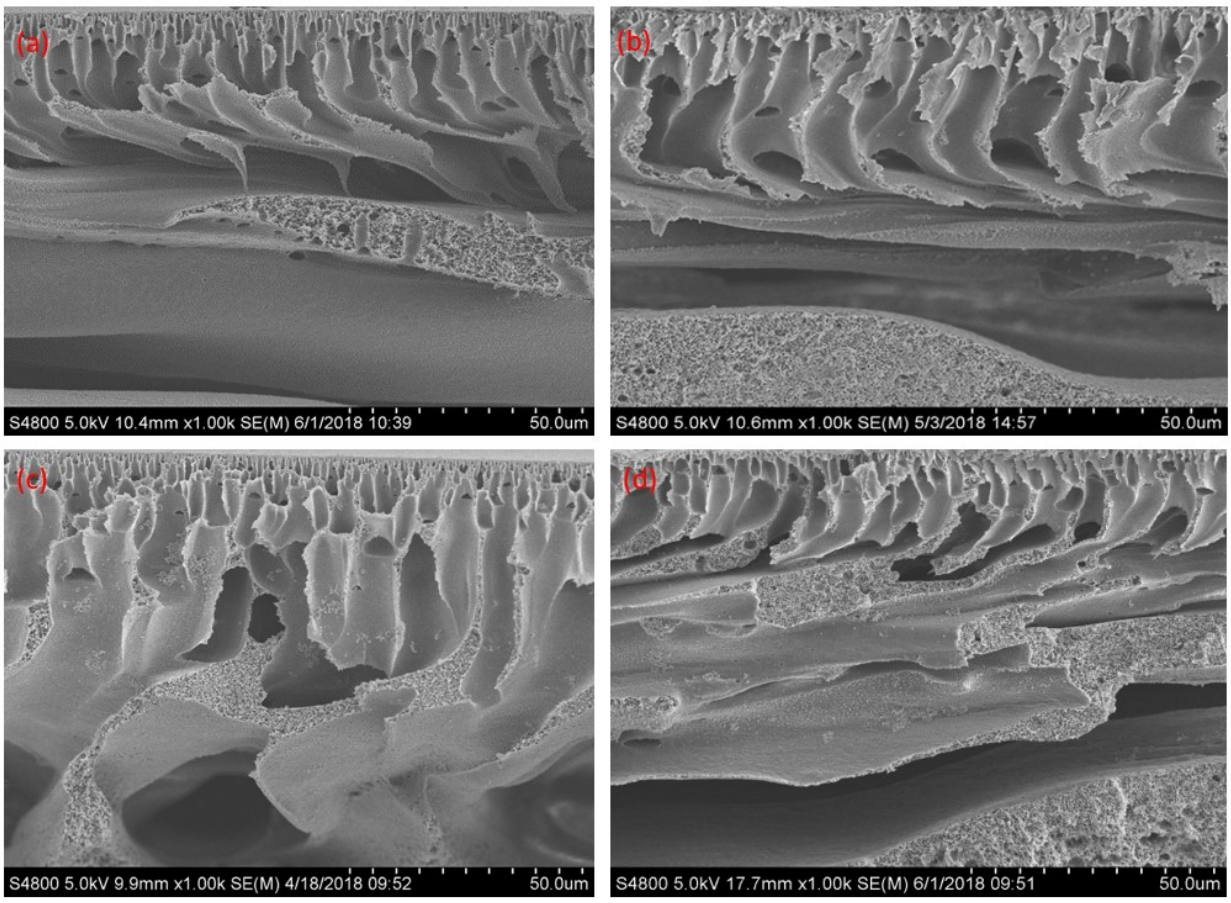


**Figure 3.1** Cross-sectional FESEM images of the prepared membranes, (a) M1: Pristine PES, (b) M2: PES-A-$Fe_3O_4$ 1wt%, (c) M3: PES-A-$Fe_3O_4$ 2wt%, (d) M4: PES-A-$Fe_3O_4$ 3wt%

NPs agglomeration was found in the cross section of membrane, mostly in the skin layer. Surface modification of NPs prevent the membrane from having the agglomeration phenomenon, but this can happen locally in the skin layer. (Figure 3.2)

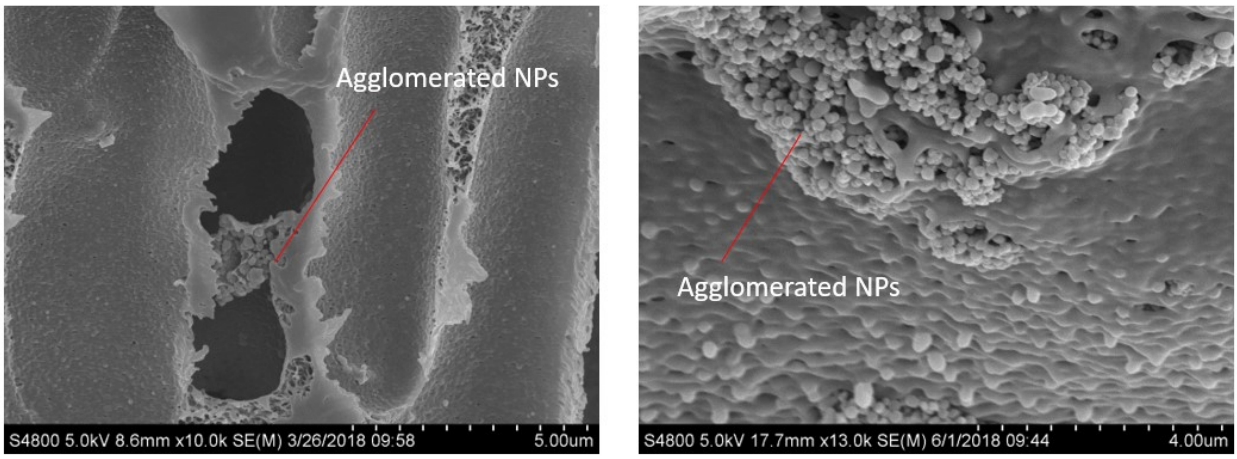


**Figure 3.2** FESEM Image of cross section of M2(left) and M4(right)

Agglomeration of NPs can block the channels, which decrease the efficiency of filtration performances. This will interfere the liquid solution flow and can possibly decrease pure water flux.

### 3.1.2 Thermal Analysis(TGA)

To examine the degree of dispersion of APTES-$Fe_3O_4$ NPs in the polymer matrix, thermogravimetric analysis (TGA) test was done on each PES-A-$Fe_3O_4$ NPs 3 times. The TGA results are shown in Figure 3.3 with its residual amount and wt. present (%). This indicates that PVP (1wt%) and PES (18wt%) were leaching out when the temperature reached into 850˚C and the residuals are composed of Iron oxide (1,2,3wt%). Assuming that all of the DMAc solvents were transferred out of the solidified PES membrane in the phase inversion process, residual weight percent of each PES-A-$Fe_3O_4$ NPs membrane (M2, M3, M4) can be expected as 5wt%, 9.5%, and 13.6%. The result from the TGA are 7.2%, 9.7%, and 14.9% (M2, M3, and M4) are shown in Table 3.1 with expected values.

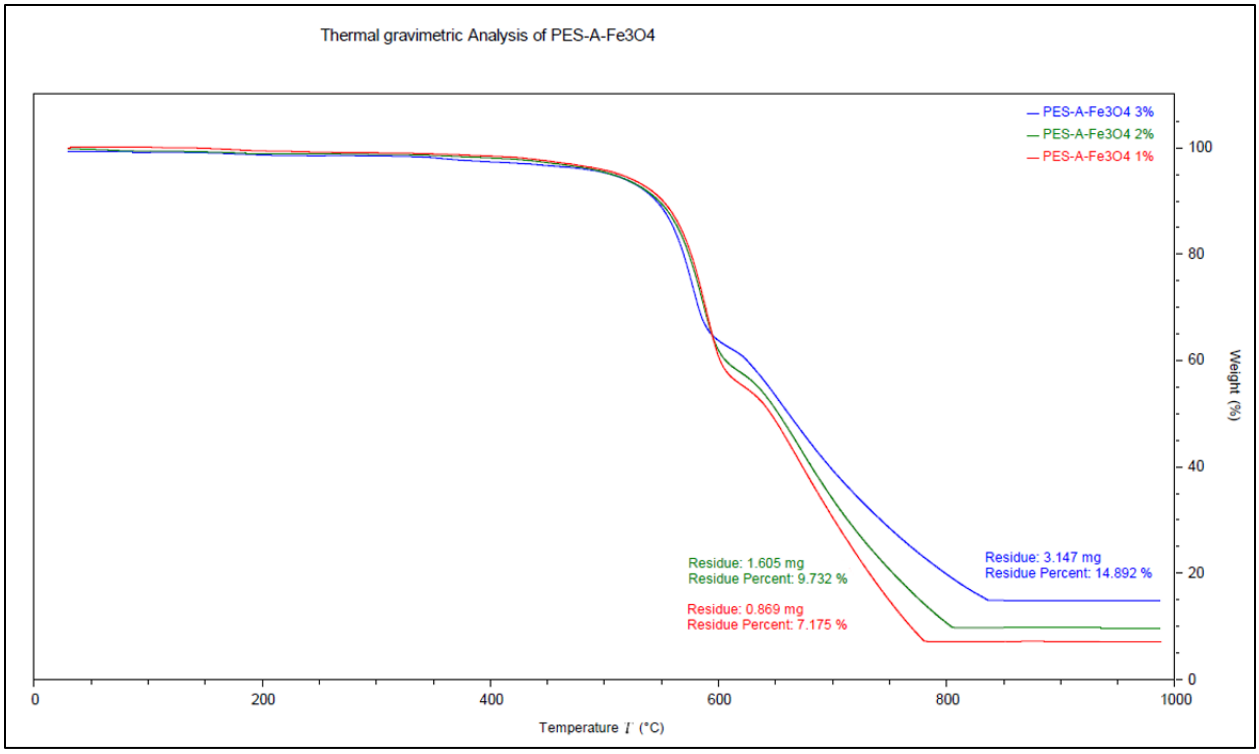


**Figure 3.3** TGA for M2, M3, M4 APTES-$Fe_3O_4$ NPs dispersion

**Table 3.1 Expected A-$Fe_3O_4$ and experimental A-$Fe_3O_4$ from TGA residual**

| Type | APTES-Fe3O4 wt. % | Expected A-Fe3O4 in Membrane(wt. %) | TGA residual (A-Fe3O4 wt. %) |
|---|---|---|---|
| M2 | 1 | 5 | 7.2 ± 0.27 |
| M3 | 2 | 9.5 | 9.7 ± 0.15 |
| M4 | 3 | 13.6 | 14.9 ± 0.07 |

With the comparison between Expected wt. % of A-$Fe_3O_4$ NPs and actual TGA results, it indicates that the modification of $Fe_3O_4$ has provided a good degree of dispersion of A-$Fe_3O_4$ in PES membranes.

### 3.1.3 Atomic Force Microscopy(AFM) and Porosity

AFM analysis was conducted to verify other characterization results. Figure 3.5 (3D) indicates all PES-A-$Fe_3O_4$ membranes AFM images which defines roughness with their bulges and valleys. The higher roughness can be gained with more up and down figures in the designated area (2μm × 2μm). These roughness values in the Table 3.2 revealed that the more NPs a nanocomposite has, it tends to have a higher value of roughness. However, M4, PES-A-$Fe_3O_4$ NPs (3wt%) shows the least roughness value and this could be explained with a somewhat smaller pore size on the surface rather than other membrane samples (M1, M2, M3)

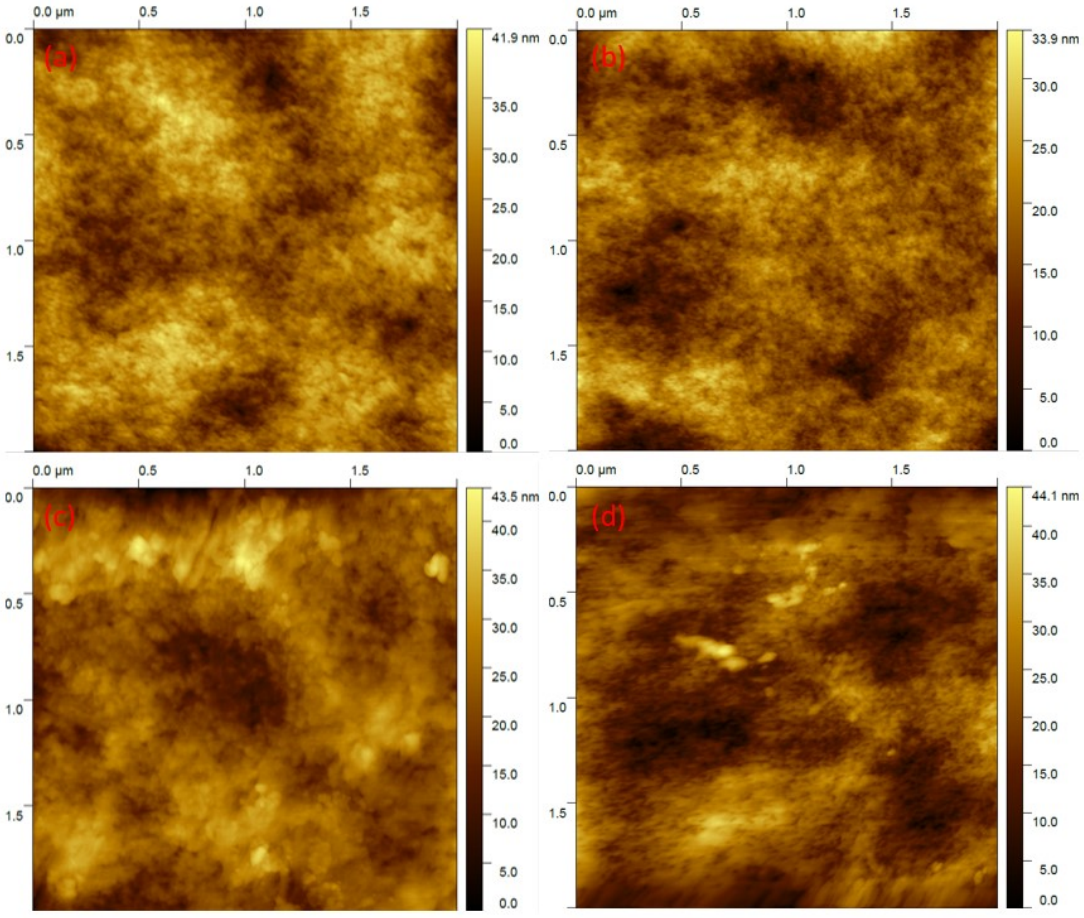


**Figure 3.4** Two dimensional(2D) AFM Image (a) M1, (b) M2, (c) M3, (d) M4

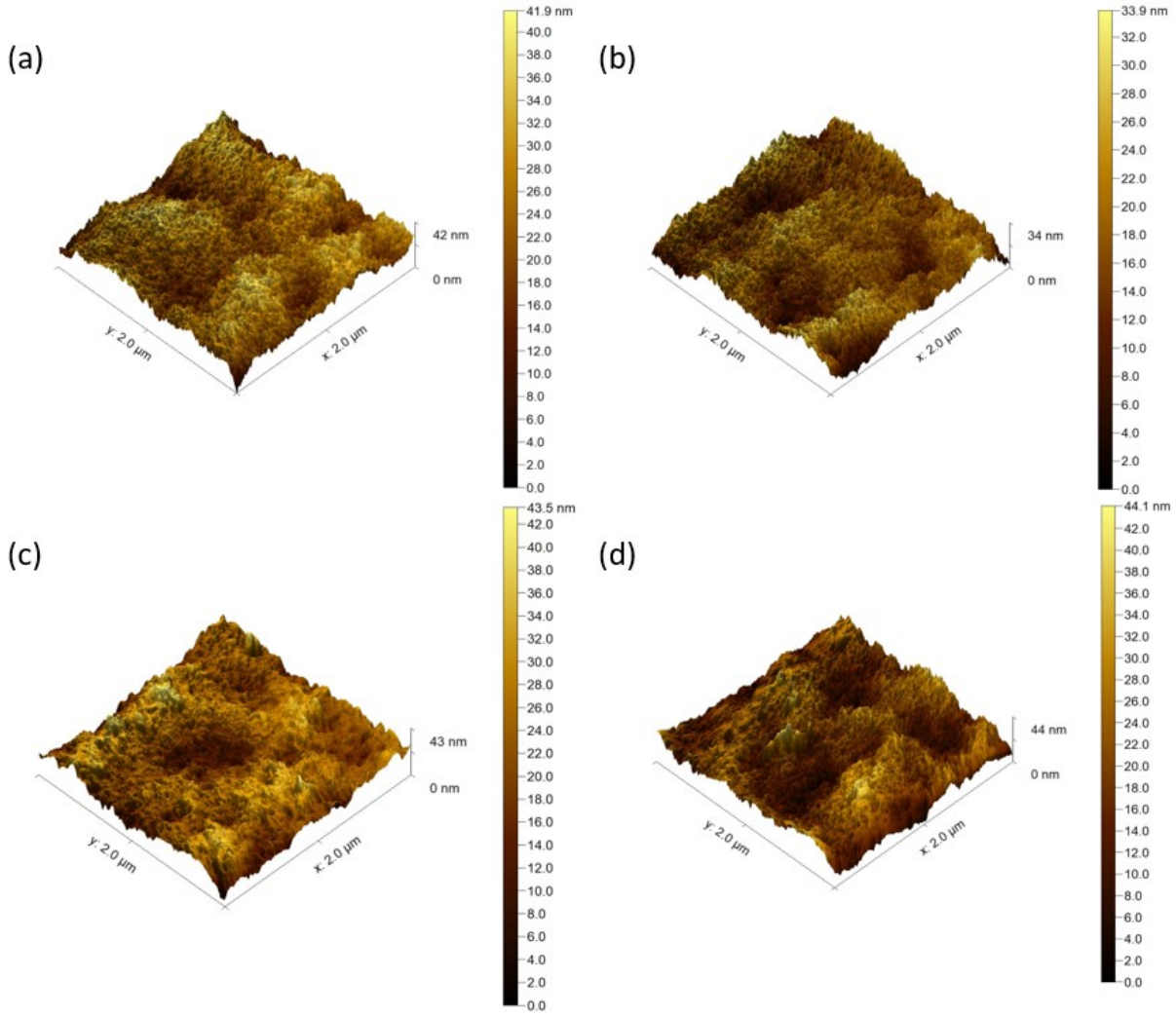


**Figure 3.5** Three dimensional(3D) AFM Image (a) M1, (b) M2, (c) M3, (d) M4

Decrease in the M4 membrane's surface roughness with more NPs can be partially caused by less agglomeration on the surface area. However, the average roughness parameter, $S_a$, shows tendency to increase with more NPs in the Membrane matrix in M1, M2, M3. This phenomenon is due to a higher chance of NPs' agglomeration, which leads to hunks in the membrane matrix. [92]

**Table 3.2 Roughness parameters, porosity, and mean porous radius of membranes.**

| Membrane Type | Roughness Parameters (nm) | | | Porosity (%) | Mean Porous radius(nm) |
|---|---|---|---|---|---|
| | $S_a$ | $S_q$ | $S_z$ | | |
| M1 | 4.08 | 5.11 | 38.5 | 0.53 | 12.13(±0.4) |
| M2 | 4.21 | 5.33 | 40.1 | 0.61 | 10.70 (±0.1) |
| M3 | 4.50 | 5.71 | 41.6 | 0.59 | 12.38(±0.2) |
| M4 | 3.51 | 4.41 | 36.7 | 0.71 | 12.15(±0.1) |

It was indicated from porosity results that addition of NPs contributed to higher percentage of pores in membranes. These results are verified from FESEM images (Figure 3.1) with more pores in skin layer and bigger micro-voids in sublayers in higher NPs wt. (%). It has been noticed that iron oxide NPs have a tendency to accumulate in the membrane surface and its superficial pores, which was mostly caused when the DI water touches the surface first in the casting process. [101] It has been found from the results in Table 3.2 that porosity is slightly decreased in M3, which could be due to the blockage of agglomerated NPs in the channels. This porosity has affected pure water flux and filtration of As(V) results. The mean porous radius increased from M2 to M4, which is in good agreement with the FESEM images (Figure 3.1). However, M2 turns out to have smaller pore size than M1 and this can be resulted by increased viscosity with addition of NPs. [64] [95]

### 3.1.4 Contact Angle Analysis

The hydrophilicity of PES-A-$Fe_3O_4$ membrane surfaces were characterized with contact angle. The larger contact angle it has, the more hydrophobic the membrane surfaces are, whereas the smaller contact angle represents a hydrophilic surface. [102] As shown in Figure 3.6, water contact angle of the membranes diminished with the addition of more A-$Fe_3O_4$ NPs. The Original PES membrane had a contact angle around 74.4˚, while the PES-A-$Fe_3O_4$ 1wt%, PES-

A-$Fe_3O_4$ 2wt%, and PES-A-$Fe_3O_4$ 3wt% showed decrease in contact angle as 70.04˚, 68.8˚, 62.9 ˚with more contents of A-$Fe_3O_4$ NPs. This indicates that hydrophilicity of PES membrane was improved with the increase of A-$Fe_3O_4$ NPs. The measurements were conducted 5 spots in each membrane sample and average values were described in the Figure 3.6. The images of water drop on each membrane were shown in the Figure 3.7 by implying more hydrophilicity of membranes with addition of A-$Fe_3O_4$ NPs.

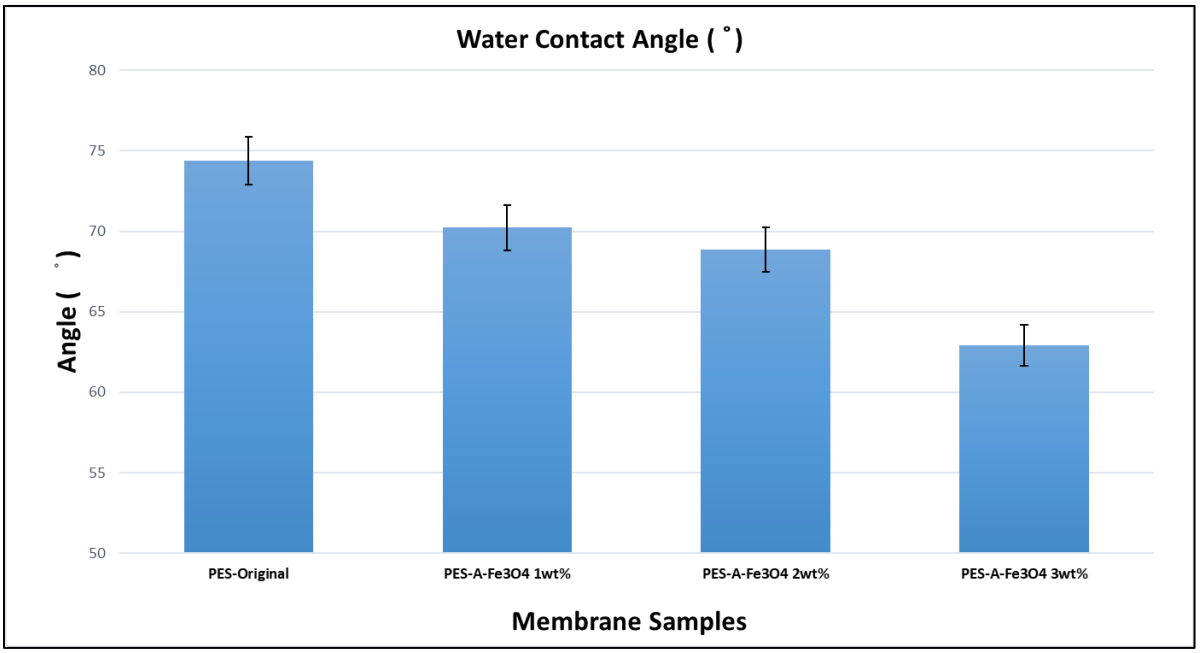


**Figure 3.6** Average Water Contact Angle of PES-A-$Fe_3O_4$ NPs membrane (0, 1, 2, 3wt. %)

The improved hydrophilicity from Figure 3.6 and Figure 3.7 can be explained with more NPs around the membrane surfaces, which was caused by the phenomenon to reduce interface energy of NPs during phase inversion process. APTES-$Fe_3O_4$ Nano composites migrate spontaneously to the surface in the membrane matrix when the DI water touches casting solutions in glass substrates.

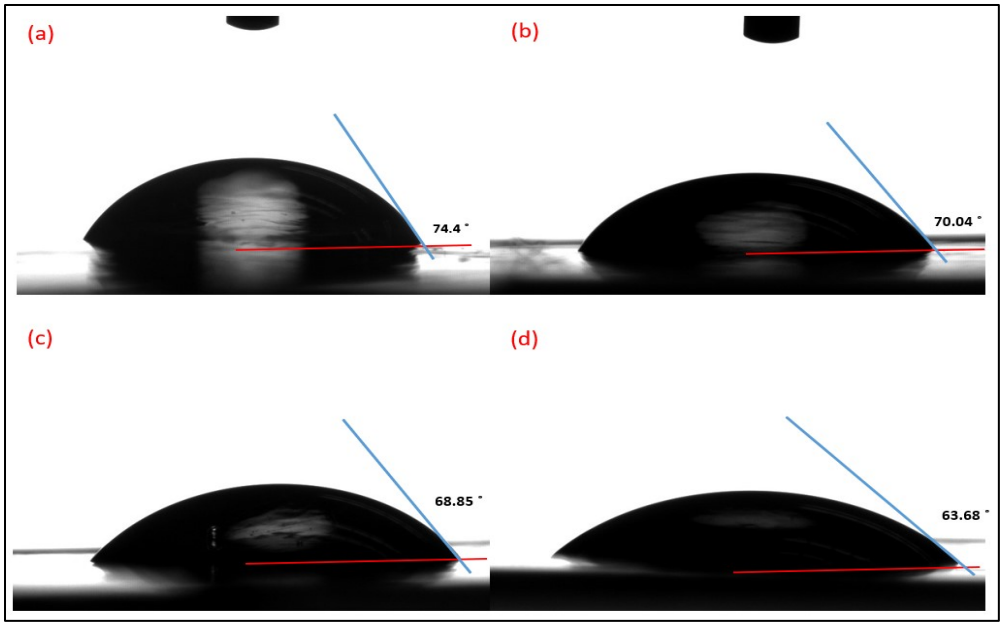


**Figure 3.7** Image from Goniometer for Water Contact Angle of each membrane sample. (a) Pristine PES, (b) PES-A-$Fe_3O_4$ 1wt%, (c) PES-A-$Fe_3O_4$ 2wt%, (d) PES-A-$Fe_3O_4$ 3wt%

The increase in hydrophilicity of Nano composite membranes was caused by the hydrophilic properties of $Fe_3O_4$ NPs and the -$NH_2$ functional group grafted on $Fe_3O_4$ NPs.

### 3.1.5 IR Analysis

To analyze the functionality of $Fe_3O_4$ NPs with APTES (Aminopropyltriethoxy silane) modification, Infrared spectroscopy (IR spectroscopy, Shimadzu IR Tracer 100) was used with the condition of 200 scans 4cm-1 Resolution for the transmittance. The Figure 3.8 indicates difference between $Fe_3O_4$ NPs and APTES modified $Fe_3O_4$ in the wavelength range from 350cm-1 to 5000cm-1. The graph (b) illustrated peaks at the band range of 2840-2960 cm-1 which represents the stretching model of alkyl (-CH2, -CH3) and another peak at the band range of 1560cm-1 which represents –NH functional group. The APTES structure is shown below in the Figure 3.9

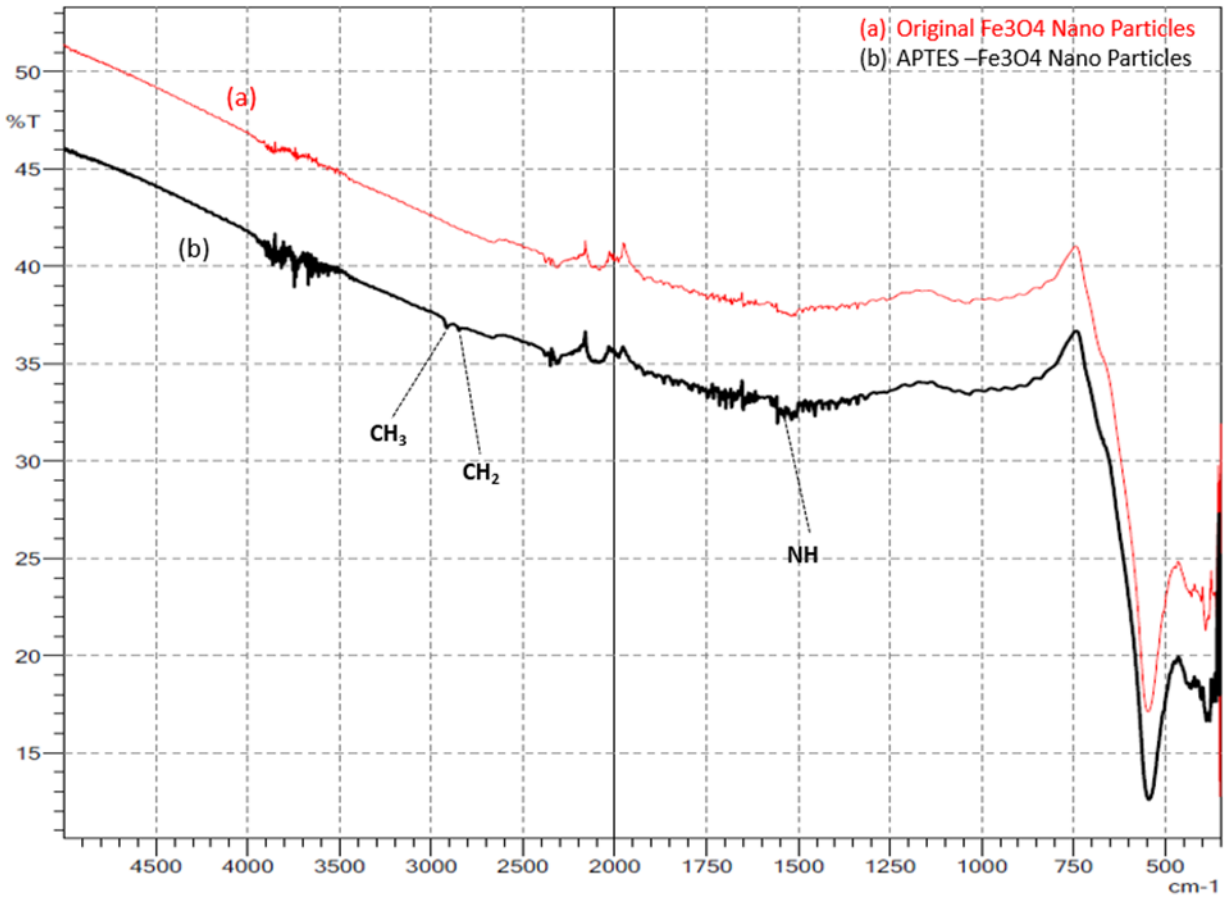


**Figure 3.8** IR spectra of unmodified (a) and APTES modified (b)

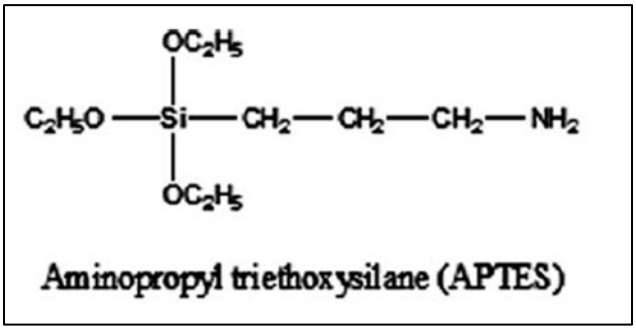


**Figure 3.9** Chemical structure of silane coupling agent (APTES) [91]

From the IR analysis, it can be ascertained that the functional silane groups are successfully grafted into $Fe_3O_4$ NPs surface.

Figure 3.10 shows the IR spectra of PES and PES-A-$Fe_3O_4$ NPs (1wt%). Even though APTES-$Fe_3O_4$ NPs was comprised as 1wt% of the whole PES-A-$Fe_3O_4$ composite membrane, relatively higher intensities of H-O-H bond at peak at the range of 3200-3700cm-1, Fe-O band(weak) at the peak of 421cm-1[103], and CH3 stretch bond anchored onto Iron oxide at the peak of 2354 cm-1 were shown in IR analysis.

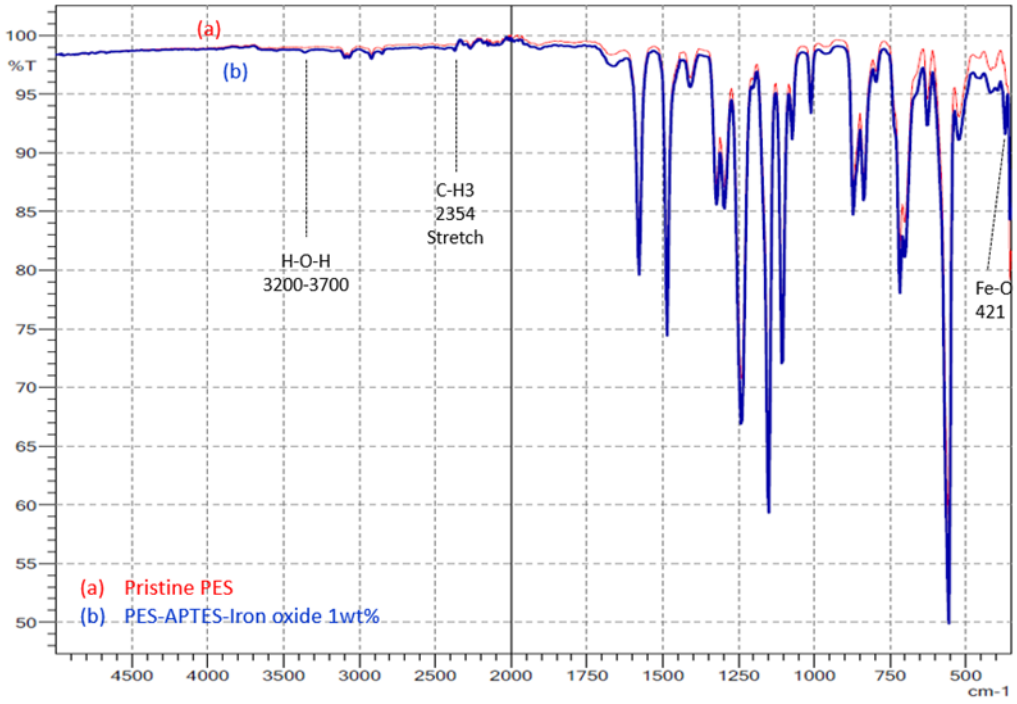


**Figure 3.10** IR spectroscopy for (a) Original PES and (b) PES-1wt% APTES-Fe3O4

For the operating IR spectroscopy of pristine PES and PES-APTES-$Fe_3O_4$, the transmittance was chosen under 100 scans and 8cm-1 resolution in the wavelength range of 350cm-1 to 5000cm-1.

### 3.1.6 TEM Analysis

To analyze the modification of $Fe_3O_4$-NPs surface, Transmission electron microscopy (TEM, Hitachi H-9000NAR microscope) was operated at 300KeV. Sample was characterized with bright field (BF) imaging for sample morphology, selected area diffraction (SAD) for crystallographic information, and high-resolution transmission electron microscopy (HRTEM) for high-mag morphology and crystallography. Modified A-$Fe_3O_4$ NPs TEM images are shown in Figure 3.11. APTES, amorphous polymer structure, were directly attached into the $Fe_3O_4$ NPs surface based on the IR characterization. Since TEM analyzes only crystalline structure of samples, Figure 3.11 does not show amorphous layer (APTES) on crystalline NPs ($Fe_3O_4$).

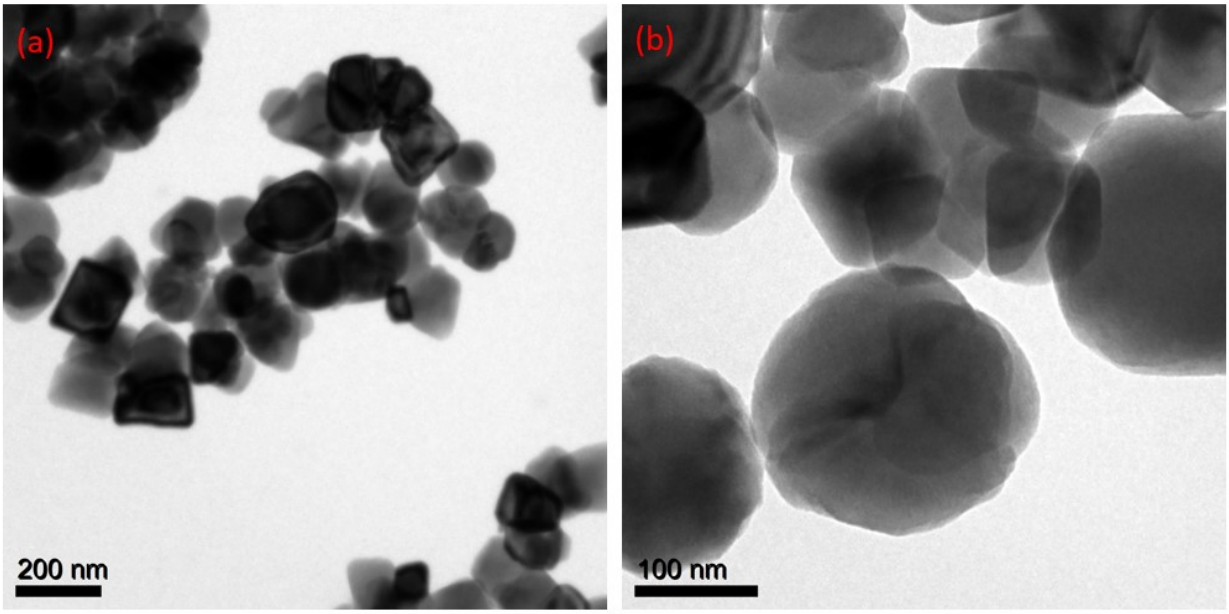


**Figure 3.11** TEM Images for APTES-$Fe_3O_4$ NPs

## 3.2 Performance Analysis

### 3.2.1 Water Flux of Membranes

Pure water flux or pure water permeability (PWP) indicates a critical parameter for the degree of porosity for membrane samples (M1, M2, M3, M4) and is directly related to the membrane pore size. [104-106] The result of pure water flux is shown from Figure 3.12 by representing the effects of adding APTES-$Fe_3O_4$ NPs on PWP results. The biggest reason for the increase in PWP of membrane samples can be the extended size of macro-voids in the sub-layer and more porous structure in the skin layer. [95] However, PES-A-Fe3O4 1wt% membrane showed less ability for filtration of solution than pristine PES membrane, this can be caused by blockage of the possible water channels or pores by APTES-$Fe_3O_4$ NPs agglomeration.

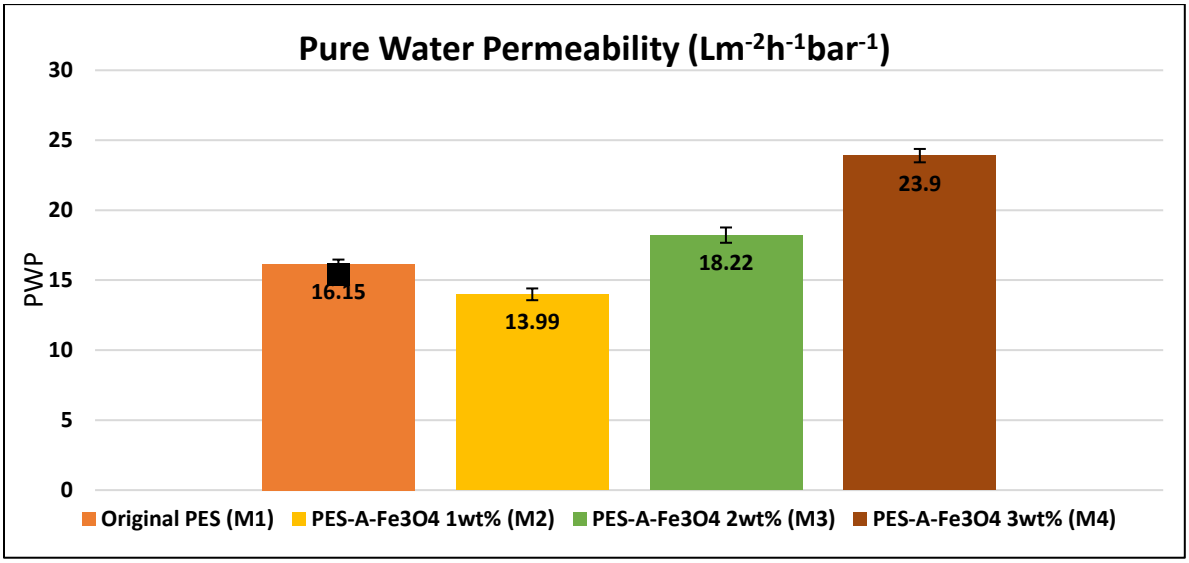


**Figure 3.12** Pure water permeability (PWP) of the prepared each sample (M1, M2, M3, M4)

### 3.2.2 Arsenic Adsorption of Membrane

3.2.2.1 Equilibrium study and adsorption isotherms

The relation between the equilibrium adsorption capacities of pristine and nanocomposite PES membranes(M1, M2, M3, M4) vs the initial concentration of As(V) solution(2ppm, 4ppm, 6ppm, 8ppm) were presented in Figure 3.2 The pristine PES membrane shows the lowest adsorption capacity close to zero for As(V) due to the absence of APTES-$Fe_3O_4$ NPs, efficient absorbent in the PES membrane matrix. On the other hand, PES nanocomposite containing APTES-$Fe_3O_4$ NPs showed an increasing tendency in absorption capacity for the increasing concentration of As(V) solution (2ppm, 4ppm, 6ppm, 8ppm) with higher chance of absorption between As(V) ions and APTES-$Fe_3O_4$ NPs. The results shown in the Figure 3.13 indicate that the adsorption capacity of PES nanocomposite increases with the addition of APTES-$Fe_3O_4$ NPs. The maximum adsorption capacity was achieved in PES-A-$Fe_3O_4$ 3wt% (M4) as the value of 14.6mg/g in the curve.

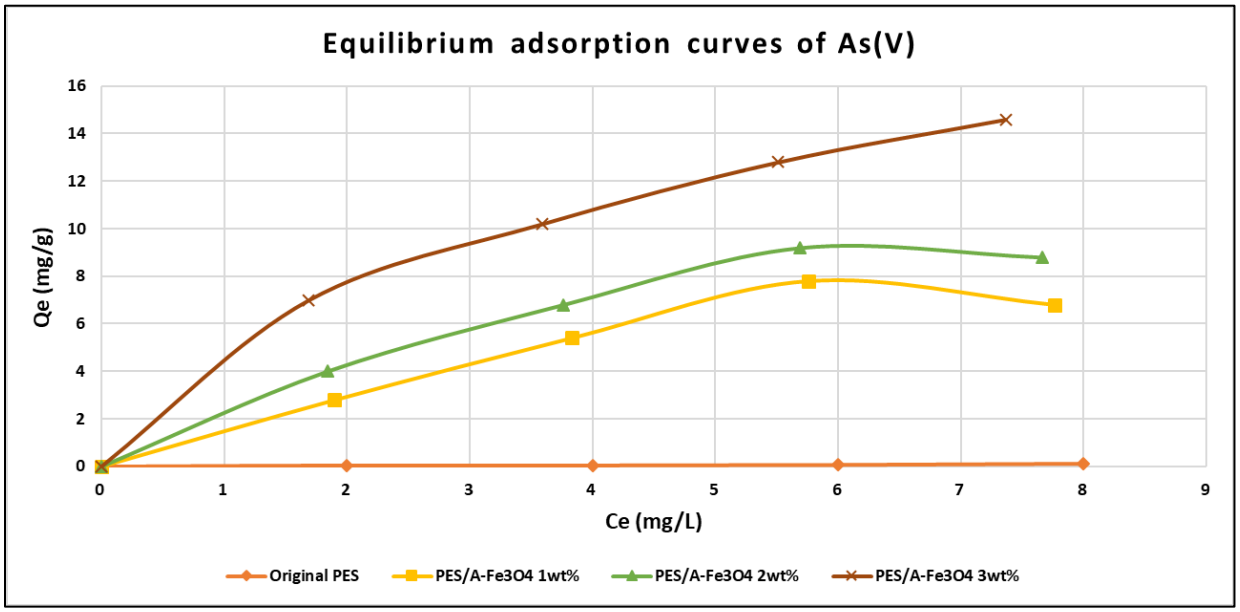


**Figure 3.13** Equilibrium adsorption curves of As(V) : Qe

For the equilibrium adsorption curves of As(V) solution (2ppm, 4ppm, 6ppm, 8ppm), two types of isothermal models, Langmuir and Freundlich were applied with the equations below.

$$\frac{1}{Q} = \frac{1}{K_L C_e Q_{max}} + \frac{1}{Q_{max}} \tag{6}$$

where $C_e$ is the arsenic concentration in solution(mg/L), $Q_{max}$ is maximum adsorption value for capacity(mg/g), and $K_L$ is the Langmuir adsorption constant(L/mg). $Q_{max}$ and $K_L$ can be determined by the intercept and the slope of $\frac{1}{Q}$ vs $\frac{1}{C_e}$ curve, distinctively,

$$\log Q = \log K_F + \frac{1}{n} \log C_e \tag{7}$$

where, $K_F$ is the Freundlich constant and n is the heterogeneity factor. All the constants for both of the equations were calculated by the linear regression of each isotherms and the obtained values are listed in Table 3.3. Each equation's $R^2$ values demonstrate that Langmuir adsorption isotherm is more suitable to show the adsorption isotherm of As(V) for PES-A-$Fe_3O_4$ NPs. Since Langmuir isotherm is a traditional model for adsorption phenomena on a homogeneous surface while Freundlich isotherm is adsorption model for heterogeneous surface, the results for $R^2$ value suggest that the adsorption between surface and adsorbate takes place at specific homogeneous spots in PES-A-$Fe_3O_4$ NPs membranes assuming a molecule occupies a single spot. [108] However, the more contents of NPs the membrane has, the adsorption tends to take place more in heterogeneous surface by having higher $R^2$ value in Freundlich isotherm model. These were confirmed by the plot of Langmuir isotherm equation (6) and Freundlich isotherm equation (7) in the Figure 3.14 and Figure 3.15.

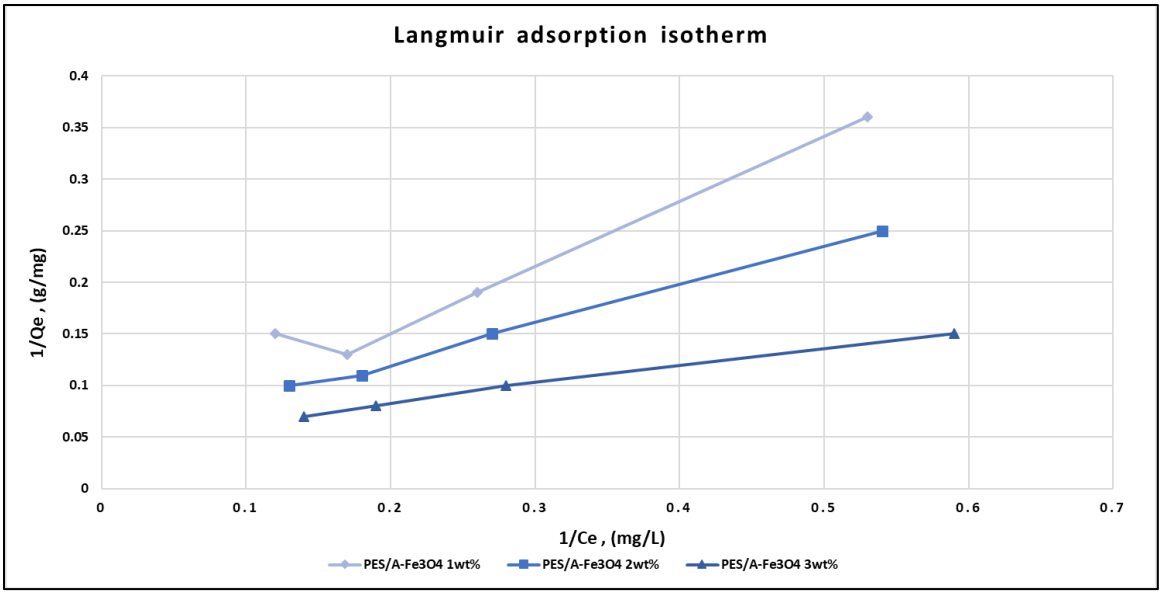


**Figure 3.14** Langmuir adsorption isotherm of nanocomposite membranes, conditions: T=25 ˚C, pH=2

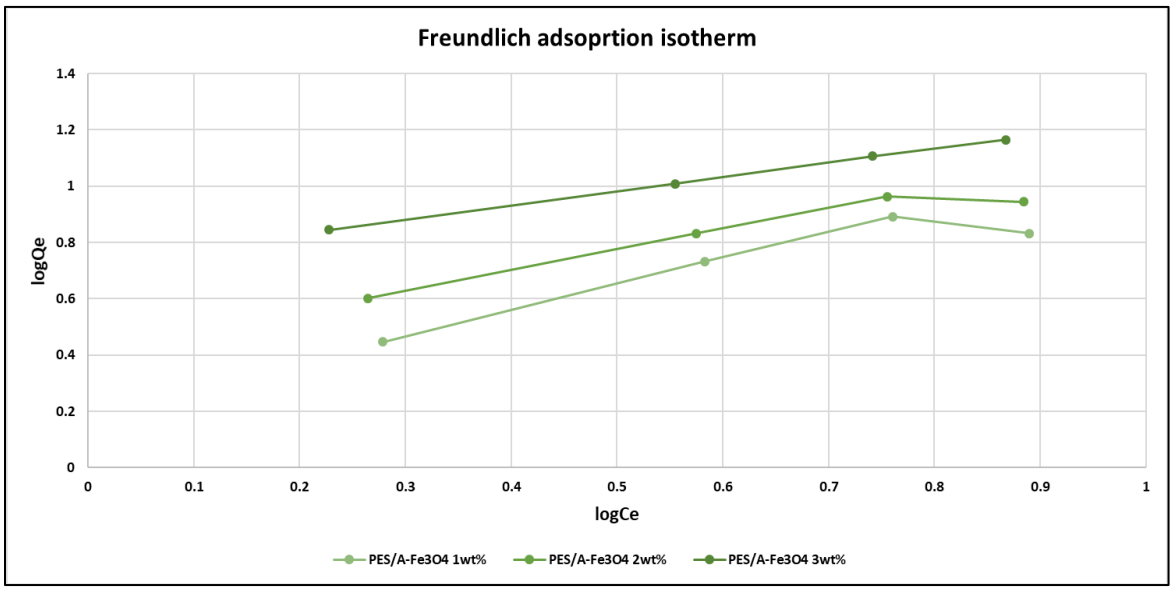


**Figure 3.15** Freundlich adsorption isotherm of nanocomposite membranes, T=25 ˚C, pH=2

**Table 3.3 Langmuir and Freundlich isotherm parameters for As(V) removal using nanocomposite membranes with different APTES-$Fe_3O_4$ contents pH=2**

| Membrane | Langmuir model | | | Freundlich model | | |
|---|---|---|---|---|---|---|
| | $K_L$(L/mg) | $Q_{max}$(mg/g) | $R^2$ | $K_F$ (mg/g) | 1/n | $R^2$ |
| PES-A-$Fe_3O_4$ 1wt% | 0.10 | 17.83 | 0.9588 | 1.93 | 0.6996 | 0.8810 |
| PES-A-$Fe_3O_4$ 2wt% | 0.13 | 20.96 | 0.9971 | 2.92 | 0.5974 | 0.9316 |
| PES-A-$Fe_3O_4$ 3wt% | 0.27 | 21.19 | 0.9955 | 5.06 | 0.5028 | 0.9996 |

### 3.2.2.2. Adsorption dynamic kinetics As(V) studies of membranes

In order to study the adsorption kinetic of As(V) of prepared membrane, PES membranes with A-$Fe_3O_4$ NPs which have high removal efficiency in batch adsorption (M2, M3, M4) were tested for filtration of the synthetic 1 ppm As(V) solution, pH=7. The permeate solution through membrane cell under pressure of 50psi was collected and analyzed every 30 minutes with ICP-MS-2030, Shimazu, Japan. The permeate As(V) concentration and As(V) rejection in the Figure 3.16 and Figure 3.17 show that As(V) adsorption continues until it reaches 210 mins having a 70±6 % rejection. After 210mins, all the prepared membranes' (M2, M3, M4) results indicate that the adsorption capacity decreases rapidly and reaches its equilibrium at 270mins. These observations can be attributed to the saturation of accessible bonding sites of A-$Fe_3O_4$ NPs by previously adsorbed As(V) ions. For the membrane samples (M2, M3, M4), It was found that the more A-$Fe_3O_4$ NPs it contains, the higher As(V) rejections and filtration performance it has during the kinetic adsorption experimentation.

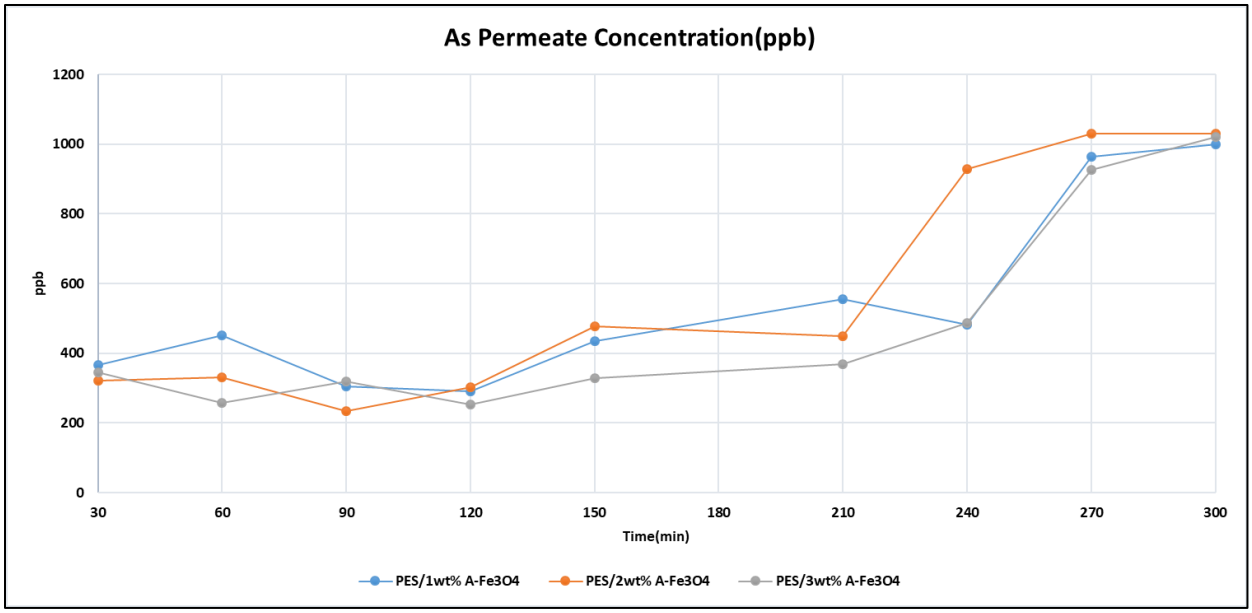


**Figure 3.16** Prepared Membranes (M2, M3, M4) As(V) ion Permeate Concentration at 50psi

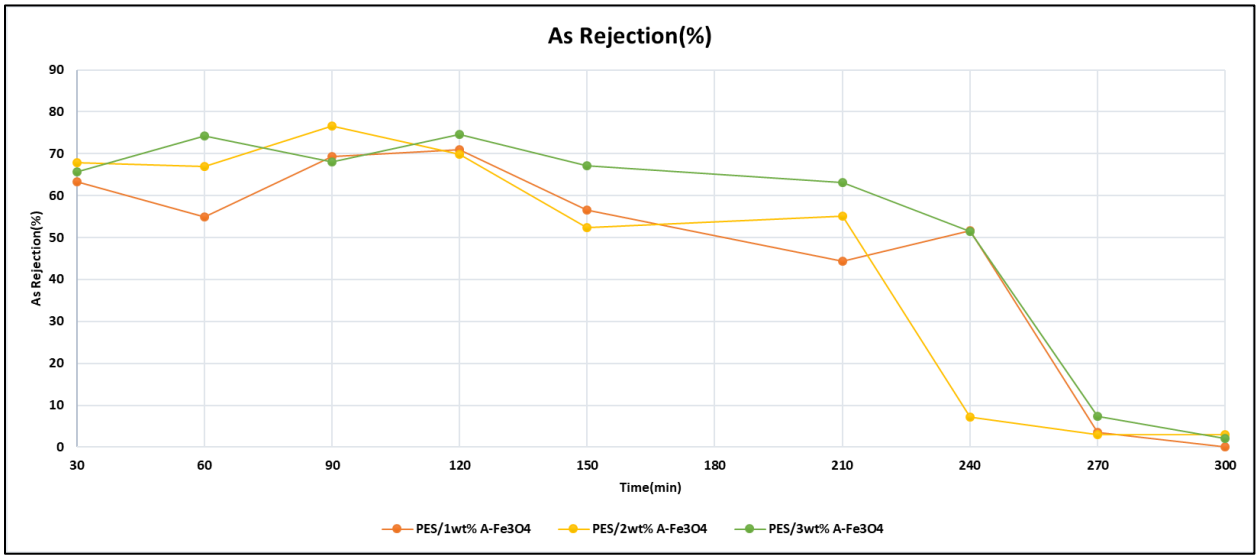


**Figure 3.17** Prepared Membranes (M2, M3, M4) As(V) ion rejection at 50psi

# CHAPTER4

# CONCLUSION

Novel polyethersulfone membranes were prepared with surface modified APTES-$Fe_3O_4$ NPs to remove arsenate ions from drinking water or industrial waste.

Several conclusions can be made from the experimental work as listed below.

1. **TGA analysis results for each prepared membrane samples (M2, M3, M4) verify that treated nano particles were well-dispersed in the PES membrane.** The characterization of nano particles using IR spectroscopy proved that Fe3O4 NPs were surface treated by showing transmittance peak around 2840-2960 cm-1 wavelength for alkyl group stretch and another peak around 1560 cm-1 wavelength for -NH group for grafted APTES molecules.

2. **The addition of A-$Fe_3O_4$ NPs caused more porous structure and smaller size pore in skin layer.** Atomic Force Microscopy shows the difference in roughness between the samples by indicating that A-$Fe_3O_4$ NPs contributed in the formation of rougher surface until more than 2wt % A-$Fe_3O_4$ NPs was added. Membrane with 3wt% A-$Fe_3O_4$ NPs showed least roughness among samples with smaller pore size on the surface area. Pore structure image of membrane cross-section was analyzed by FESEM. It was found in FESEM that sub-layer has extended size of micro-void by adding more A-$Fe_3O_4$ NPs.

3. **Membrane pore percentage was increased by addition of A-$Fe_3O_4$ NPs.** Mean pore size has a tendency to increase with more contents of A-$Fe_3O_4$ NPs, which is due to higher viscosity. Sub-layer micro-void size with different A-$Fe_3O_4$ NPs weight percent affected pure water flux value. Pure PES membrane shows better performance than PES-A-$Fe_3O_4$ NPs 1wt% because agglomeration phenomena is more dominant than enlarged sub-layers pore structure effect. However, for the cases of M3 and M4, which include 2wt% and 3wt% A-$Fe_3O_4$ NPs, it has been found that pure water flux performance is inclined to be higher when adding more NPs.

4. **Addition of A-Fe3O4 NPs improves hydrophilicity.** Contact analysis of PES-A-$Fe_3O_4$ NPs measured verify that the lowest value of contact angle and highest hydrophilicity were observed from the sample M4 (PES-A-$Fe_3O_4$ 3wt%).

5. The prepared PES-A-Fe3O4 NPs nanocomposite membrane showed an increasing trend in adsorption capacity with higher concentration of As(V) solution, while pure PES membrane shows nearly zero adsorption capacity as was revealed by the batch adsorption test.

6. **The adsorption capacity decreases dramatically for all of three membranes samples (M2, M3, M4) at 210 mins.** In adsorption dynamic kinetics for As(V) adsorption test under pressure, 50psi with 1ppm As(V) , pH=7 solution, PES-A-$Fe_3O_4$ 3wt% (M4) showed a little of higher As(V) removal percentage than PES-A-$Fe_3O_4$

1wt% (M3) PES-A-$Fe_3O_4$ and 2wt% (M2). M2 and M3 values showed similar As(V) removal percentage. All of these three membrane samples (M2, M3, M4) removed 70±6% of As(V) from feed until it reached equilibrium point at 270 mins.

# REFERENCES


[1] Audi, G., Bersillon, O., Blachot, J. and Wapstra, A.H. (2003) The NUBASE evaluation of nuclear and decay properties. Nuclear Physics A, 729(1), 3–128

[2] Faure, G. (1998) Principles and Applications of Geochemistry, 2nd edn, Prentice Hall, Upper Saddle River, NJ, p. 600.

[3] Shih, M.-C. (2005) An overview of arsenic removal by pressure-driven membrane processes. Desalination, 172(1), 85–97.

[4] Klein, C. (2002) The 22nd Edition of the Manual of Mineral Science (after James D. Dana), John Wiley & Sons, Inc., New York, p. 641.

[5] Foster, A.L. (2003) Spectroscopic investigation of arsenic species in solid phases, in Arsenic in Ground Water (eds A.H. Welch and K.G. Stollenwerk), Kluwer Academic Publishers, Boston, MA, pp. 27–65.

[6] Francesconi, K.A., Edmonds, J.S. and Morita, M. (1994) Determination of arsenic and arsenic species in marine environmental samples, in Arsenic in the Environment: Part I: Cycling and Characterization (ed. J.O. Nriagu), John Wiley & Sons, Inc., New York, pp. 189–219.

[7] Pokrovski, G., Gout, R., Schott, J. et al. (1996) Thermodynamic properties and stoichiometry of As(III) hydroxide complexes at hydrothermal conditions. Geochimica et Cosmochimica Acta, 60(5), 737–49.

[8] Yokoyama, T., Takahashi, Y. and Tarutani, T. (1993) Simultaneous determination of arsenic and arsenious acids in geothermal water. Chemical Geology, 103(1-4), 103–11.

[9] Price, R.E. and Pichler, T. (2005) Distribution, speciation and bioavailability of arsenic in a shallow-water submarine hydrothermal system, Tutum Bay, Ambitle Island, PNG. Chemical Geology, 224(1-3), 122–35.

[10] Henke, K. (2009). Arsenic: Environmental Chemistry, Health Threats and Waste Treatment, John Wiley & Sons, pp. 0-66

[11] Stollenwerk, K.G. (2003) Geochemical processes controlling transport of arsenic in groundwater: a review of adsorption, in Arsenic in Ground Water (eds A.H. Welch and K.G. Stollenwerk), Kluwer Academic Publishers, Boston, MA, pp. 67–100.

[12] Gr¨afe, M. and Sparks, D.L. (2006) Solid phase speciation of arsenic, in Managing Arsenic in the Environment: From Soil to Human Health (eds R. Naidu, E. Smith, G. Owens et al.), CSIRO Publishing, Collingwood, pp. 75–91.

[13] Craig, P.J., Eng, G. and Jenkins, R.O. (2003) Occurrence and pathways of organometallic compounds in the environment — general considerations, in Organometallic Compounds in the Environment, 2nd edn (ed. P.J. Craig), John Wiley & Sons, Ltd, West Sussex, pp. 1–55.

[14] Schreiber, M.E., Gotkowitz, M.B., Simo, J.A. and Freiberg, P.G. (2003) Mechanisms of arsenic release to water from naturally occurring sources, eastern Wisconsin, in Arsenic in Ground Water (eds A.H., Welch and K.G. Stollenwerk), Kluwer Academic Publishers, Boston, MA, pp. 259–80.

[15] Smedley, P.L., Nicolli, H.B., Macdonald, D.M.J. et al. (2002) Hydrogeochemistry of arsenic and other inorganic constituents in groundwaters from La Pampa, Argentina. Applied Geochemistry, 17(3), 259–84.

[16] Redman, A.D., Macalady, D.L. and Ahmann, D. (2002) Natural organic matter affects arsenic speciation and sorption onto hematite. Environmental Science and Technology, 36(13), 2889–96.

[17] https://www.bgs.ac.uk/arsenic , accessed on 09-29-2018 at 1:10 PM

[18] Gaus, I., Kinniburgh, D.G., Talbot, J.C. and Webster, R. (2003) Geostatistical analysis of arsenic concentration in groundwater in Bangladesh using disjunctive kriging. Environmental Geology, 44(8), 939–48.

[19] K. Jomova, Z. Jenisova, M. Feszterova, S. Baros, J. Liska, D. Hudecova, C. J. Rhodesd and M. Valkoc, (2011) Arsenic : toxicity, oxidative stress and human disease, Journal of Applied Toxicology, 31:95-107

[20] Gorby, S. (1988). Arsenic poisoning. Western Journal of Medicine, 149, 308-315.

[21] Greenfield, G. (2004). Agent Blue and the business of killing rice. *Ecologist*, https://www.countercurrents.org/us-greenfield180604.htm, accessed on 01-24-2018

[22] Vahter, M. and Norin, H. (1980) Metabolism of 74As-labeled trivalent and pentavalent inorganic arsenic in mice. Environmental Research, 21(2), 446–57.

[23] Eby, G.N. (2004) Principles of Environmental Geochemistry, Thomson Brooks/Cole, Pacific Grove, CA, p. 514.

[24] Fetter, C.W. (1993) Contaminant Hydrogeology, Prentice Hall, Upper Saddle River, NJ, p. 458.

[25] US Environmental Protection Agency (US EPA) (2002b) Proven Alternatives for Aboveground Treatment of Arsenic in Groundwater. EPA-542-S-02-002, Office of Solid Wastes and Emergency (5102G).

[26] Kim, Y., Kim, C., Choi, I. et al. (2004) Arsenic removal using mesoporous alumina prepared via a templating method. Environmental Science and Technology, 38(3), 924–31.

[27] Mayo, J.T., Yavuz, C., Yean, S. et al. (2007) The effect of nanocrystalline magnetite size on arsenic removal. Science and Technology of Advanced Materials, 8, 71–75.

[28] Ndur, S.A. and Norman, D.J. (2003) Sorption of arsenic onto laterite: a new technology for filtering rural water. Abstracts with Programs - Geological Society of America, 35(6), 413.

[29] Cumbal, L. and Sengupta, A.K. (2005) Arsenic removal using polymer-supported hydrated iron(III) oxide nanoparticles: Role of Donnan membrane effect. Environmental Science and Technology, 39(17), 6508–15.

[30] http://www.earthpigments.com/black-iron-oxide-pigment/, accessed on 1-25-2018

[31] Clifford, D.A. and Ghurye, G.L. (2002) Metal-oxide adsorption, ion exchange, and coagulation-microfiltration for arsenic removal from water, in Environmental Chemistry of Arsenic (ed. W.T. Frankenberger Jr.), Marcel Dekker, New York, pp. 217–45.

[32] Hlavay, J. and Poly´ak, K. (2005) Determination of surface properties of iron hydroxide-coated alumina adsorbent prepared for removal of arsenic from drinking water. Journal of Colloid and Interface Science, 284(1), 71–77.

[33] Pal, P., Ahammad, Z. and Bhattacharya, P. (2007) ARSEPPA: a visual basic software tool for arsenic separation plant performance analysis. Chemical Engineering Journal, 129(1-3), 113–22.

[34] Spellman, F.R. (2003) Handbook of Water and Wastewater Treatment Plant Operations, Lewis Publishers, Boca Raton, FL, p. 661.

[35] Bothe, J.V., Jr. and Brown, P.W. (1999) Arsenic immobilization by calcium arsenate formation. Environmental Science and Technology, 33(21), 3806–11.

[36] Jekel, M.R. (1994) Removal of arsenic in drinking water treatment, in Arsenic in the Environment: Part I: Cycling and Characterization (ed. J.O. Nriagu), John Wiley & Sons, Inc., New York, pp. 119–32.

[37] Hering, J.G., Chen, P.-Y., Wilkie, J.A. and Elimelech, M. (1997) Arsenic removal from drinking water during coagulation. Journal of Environmental Engineering, 123(8), 800–7.

[38] Brandhuber, P. and Amy, G. (1998) Alternative methods for membrane filtration of arsenic from drinking water. Desalination, 117(1-3), 1–10.

[39] http://www.toltec.biz/how_hemodialysis_works.htm, accessed on 01-29-2018

[40] Simona Caprarescua, Anita-Laura Radub, Violeta Purcarb. et al, (2015) Adsorbents/ion exchangers-PVA blend membranes: Preparation characterization and performance for the removal of Zn 2+ by electrodialysis, Applied Surface Science 329, 65-75

[41] Anirudhan, T.S. and Unnithan, M.R. (2007) Arsenic(V) removal from aqueous solutions using an anion exchanger derived from coconut coir pith and its recovery. Chemosphere, 66(1), 60–66.

[42] Chen, C.-C. and Chung, Y.-C. (2006) Arsenic removal using a biopolymer chitosan sorbent. Journal of Environmental Science and Health, Part A: Toxic/Hazardous Substances and Environmental Engineering, 41(4), 645–58.

[43] Mokashi, S.A. and Paknikar, K.M. (2002) Arsenic (III) oxidizing Microbacterium lacticum and its use in the treatment of arsenic contaminated groundwater. Letters in Applied Microbiology, 34(4), 258–62, Erratum: 35(2), 171.

[44] Katsoyiannis, I.A. and Zouboulis, A.I. (2004) Application of biological processes for the removal of arsenic from groundwaters. Water Research, 38(1), 17–26.

[45] Mulligan, C.N., Yong, R.N. and Gibbs, B.F. (2001) Remediation technologies for metal-contaminated soils and groundwater: an evaluation. Engineering Geology, 60(1-4), 193–207.

[46] Hu, Y., Li, J.-H., Zhu, Y.-G. et al. (2005) Sequestration of as by iron plaque on the roots of three rice (Oryza sativa L.) cultivars in a low-P soil with or without P fertilizer. Environmental Geochemistry and Health, 27(2), 169–76.

[47] Montes-Bay´on, M., Meija, J., LcDuc, D.L. et al. (2004) HPLC-ICP-MS and ESI-Q-TOF analysis of biomolecules induced in Brassica juncea during arsenic accumulation. Journal of Analytical Atomic Spectrometry, 19(1), 153–58.

[48] Pratas, J., Prasad, M.N.V., Freitas, H. and Conde, L. (2005) Plants growing in abandoned mines of Portugal are useful for biogeochemical exploration of arsenic, antimony, tungsten and mine reclamation. Journal of Geochemical Exploration, 85(3), 99–107.

[49] US Environmental Protection Agency (US EPA) (2002a) Arsenic Treatment Technologies for Soil, Waste, and Water. EPA-542-R-02-004, Office of Solid Wastes and Emergency (5102G).

[50] Mulligan, C.N., Yong, R.N. and Gibbs, B.F. (2001) Remediation technologies for metal-contaminated soils and groundwater: an evaluation. Engineering Geology, 60(1-4), 193–207.

[51] Smith, L.A., Means, J.L., Chen, A. et al. (1995) Remedial Options for Metals-Contaminated Sites, CRC Lewis Publishers, Boca Raton, FL.

[52] Leist, M., Casey, R.J. and Caridi, D. (2000) The management of arsenic wastes: problems and prospects. Journal of Hazardous Materials, 76(1), 125–38.

[53] Kim, S.-O., Kim, W.-S. and Kim, K.-W. (2005) Evaluation of electrokinetic remediation of

arsenic-contaminated soils. Environmental Geochemistry and Health, 27(5-6), 443–53.

[54] Weinheim (2006)., Presently Available Membranes for Liquid Separation. In B.B. Suzana Pereira Nunes ; Klaus-Viktor Peinemann(Ed.), Membrane Technology in the Chemistry Industry, WILEY-VCH Verlag GmbH & Co. KGaA, pp. 15-38

[55] W. J. Wrasidlo (Brunswick) Asymmetric membranes. US Patent 4629563, December 1986.

[56] M. Kraus, M. Heisler, I. Katsnelson, D. Velazques (Gelman) Filtration membranes and method of making the same. US Patent 4900449, February 1990.

[57] Nicholas P Cheremisinoff. (1998) Advanced polymer processing operations. Westwood, N.J., U.S.A. : Noyes Publications, pp. 69-99

[58] Kun Qi, PhD. Dissertation, Chengdu University of Science and Technology, Chengdu, China, 1992.

[59] Z. Zhang, S.Lai, W. Wang and R. Huang. China Plastics (Chinese), 4(2), 48(1990).

[60] http://studylib.net/doc/18766171/polyarylsulfones--psu--pesu--ppsu- , accessed on 02-01-2018

[61] Jean-Francois Blanco, Julie Sublet, Quang Trong Nguyena, Pierre Schaetzel (2006)., Formation and morphology studies of different polysulfones-based membranes made by wet phase inversion process. Journal of Membrane Science 283 (27-37)

[62] P. Pardon, P. J. Hendra and H. A. Willis, Plastics Rubber and Composites Processing and Applications, 20(5), 271( 1993).

[63] J. Muras, and Z. Zamorsky, Plaste und Kaut., 32, 302(1985).

[64] S. Zinadini, A.A. Zinatizadeha, M. Rahimi, V. Vatanpour, H. Zangeneha, M. Beygzadeh (2014)., Novel high flux antifouling nanofiltration membranes for dye removal containing carboxymethyl chitosan coated Fe3O4 nanoparticles. Desalination 349 (145-154)

[65] K. C. Khulbe, C. Y. Feng, Takeshi Matsuura (2008)., Synthetic Polymeric Membranes: Characterization by Atomic Force Microscopy, Springer-Verlag Berlin Heidelberg, pp.1-14

[66] Ioannis A. Katsoyiannis et al. (2002), Removal of arsenic from contaminated water sources by sorption onto iron-oxide-coated polymeric materials. Water Research 36 (5141-5155)

[67] Qigang Chang et al. (2010), Preparation of iron-impregnated granular activated carbon for arsenic removal from drinking water

[68] Gimenez, J., Martınez, M., Pablo, J., Rovira, M., and Duro, L. (2007), ‘‘Arsenic sorption

onto natural hematite, magnetite and goethite.'' Journal of Hazardous Materials, 141, pp. 575–580.

[69] Raven, K. P., Jain, A., and Loeppert, R. H. (1998), ''Arsenite and arsenate adsorption on ferrihydrite: Kinetics, equilibrium, and adsorption envelopes.'' Environmental Science and Technology, 32, pp. 344–349.

[70] Singh, D. B., Prasad, G., and Rupainwar, D. C. (1996), ''Adsorption technique for the treatment of As(V)-rich effluents.'' Colloids and Surfaces A: Physicochemical and Engineering Aspects, 111, pp. 49–56.

[71] Mamindy-Pajany, Y., Hurel, Ch., Marmier, N., and Romeo, M. (2009), ''Arsenic adsorption onto hematite and goethite.'' Comptes Rendus Chimie, 12, pp. 876–881.

[72] Guo, H., Stuben, D., and Berner, Z. (2007), ''Removal of arsenic from aqueous solution by natural siderite and hematite.'' Applied Geochemistry, 22, pp. 1039–1051.

[73] Narahari Mahanta and Suresh Valiyaveettil (2013), "Functionalized poly (vinyl alcohol) based nanofibers for the removal of arsenic from water" RSC Advances, 3, 2776-2783

[74] V. Thavasi, G. Singh and S. Ramakrishna, Energy Environ. Sci., 2008, 1, 205–221.

[75] N. Mahanta, Y. Teow and S. Valiyaveettil, J. Nanosci. Nanotechnol., 2012, 12, 6156–6162.

[76] R. B. Hernandez, A. P. Franc, O. R. Yola, A. Lopez-Delgado, J. Felcman, M. A. L. Recio and A. L. R. Merce, J. Mol. Struct., 2008, 877, 89–99.

[77] Sarita Kango, Susheel Kalia, Annamaria Celli, James Njuguna, Youssef Habibi, Ragesh Kumar, Surface modification of inorganic nanoparticles for development of organic-inorganic nanocomposites-A review (2013), Progress in Polymer Science, 38, 1232-1261

[78] Seeram Ramakrishna Zuwei ma, Takeshi Matsuura, Polymer membranes biotechnology Preparation, Functionalization and application, Imperial College Press (2011)., pp.1-45

[79] https://www.shokubai.co.jp/en/products/functionality/pvp.html, accessed on 07-03-2018

[80] Lucie Y. Lafreniere, Frank D. F. Talbot, Takeshi Matsuura and Srinivasa Sourirajan, Effect of polyvinylpyrrolidone Additive on the performance of Polyethersulfone Ultrafiltration Membranes. Ind. Eng. Chem. Res/ 1987, 26, 2385-2389

[81] S. S. Madaeni and A. Rahimpour, Effect of type of solvent and non-solvents on morphology and performance of polysulfone and polyethersulfone ultrafiltration membranes for milk concentration (2005), Polym. Adv. Technol, 16, 717-724

[82] https://www.eastman.com/Pages/ProductHome.aspx?product=71103648, accessed on 07-

05-2018

[83] https://www.sigmaaldrich.com/catalog/product/aldrich/637106?lang=en&region=US, accessed on 07-05-2018

[84] An-Hui Lu, E. L. Salabas, and Ferdi Schuth, Magnetic Nanoparticles: Synthesis, Protection, Functionalization, and Application (2007)., Angew. Chem. Int. Ed, 46, 1222-1244

[85] S. Giri, B. G. Trewyn, M. P. Stellmaker, V. S.-Y. Lin, Stimuli-responsive controlled-release delivery system based on mesoporous silica nanorods capped with magnetic nanoparticles, Angew. Chem. Int. Ed. 2005, 44, 5038

[86] C. Bergemann, D. Muller-Schulte, J. Oster, L. Brassard, A. S. Lubbe, Magnetic ion-exchange nano- and microparticles for medical, biochemical and molecular biological applications J. Magn. Magn. Mater. 1999, 194, 45.

[87] L. Nunez, M. D. Kaminski, J. Transuranic separation using organophosphorus extractants adsorbed onto superparamagnetic carriers, Magn. Magn. Mater. 1999, 194, 102.

[88] Kyungsun Song, Wonbaek Kim, Chang-yul Suh, Dongbok Shin, Kyung-Seok Ko, Kyoochul Ha, Magnetic iron oxide nanoparticles prepared by electrical wire explosion for arsenic Removal, Powder Technology. 2013, 246, 572-574

[89] Mojun Zhu, Amria Z. Lerum, and Wei Chen, How to Prepare Reproductible, Homogeneous, and Hydrolytically Stable Aminosilane-derived layers on Silica, Langmuir. 2012, 28, 416-423

[90] Yue Liu, Yueming Li, Xue-Mei Li, and Tao He., Kinetics of (3-Aminopropyl) triethoxylesilane(APTES) silanization of Superparamagnetic Iron Oxide Nanoparticles, Langmuir. 2013, 29 (49), 15275–15282

[91] Ong Hui Lin, Hazizan Md Akil, Z.A. Mohd Ishak., Surface-Activated Nanosilica Treated With Silane Coupling Agents/Polypropylene Composites: Mechanical, Morphological, and Thermal Studies, Polymer Composites. 2011., 32, 1568-1583

[92] Parisa Daraei and Others, Novel polyethersulfone nanocomposite membrane prepared by PANI/Fe3O4 nanoparticles with enhanced performance for Cu(II) removal from water, Journal of Membrane Science 415-416 (2012) 250-259

[93] Amir Razmjou, Adhikara Resosudarmo, Rohan L. Holmes, Hongyu Li, Jaleh Mansouri, Vicki Chen., The effect of modified TiO2 nanoparticles on the polyethersulfone ultrafiltration hollow fiber membranes, Desalination 287 (2012) 271–280

[94] Russell R. Ferlita, Donald Phipps, Jana Safarik, and Daniel H. Yeh., Cryo-Snap: A Simple Modified Freeze-Fracture Method for SEM Imaging of Membrane Cross-Sections, Environmental Progress 27(2) 2008 204-209

[95] V. Vatanpour, S.S. Madaeni, L. Rajabi, S. Zinadini, A.A. Derakhshan, Boehmite nanoparticles as a new nanofiller for preparation of antifouling mixed matrix membranes, J. Membr. Sci. 401–402 (2012) 132–143.

[96] V. Vatanpour, S.S. Madaeni, A.R. Khataee, E. Salehi, S. Zinadini, H.A. Monfared, TiO2 embedded mixed matrix PES nanocomposite membranes: influence of different sizes and types of nanoparticles on antifouling and performance, Desalination 292 (2012) 19–29.

[97] https://crustal.usgs.gov/laboratories/icpms/intro.html, accessed on 07-21-2018 at 6: 42 PM

[98] A. Kashani, J. Mostaghimi. Aerosol characterization of concentric pneumatic nebulizer used in inductively coupled plasma-mass spectrometry (ICP-MS), Atomization and Sprays (2010), 20

[99] Frank Vanhaecke, Patrick Degryse, Isotopic Analysis Fundamentals and Applications Using ICP-MS, 2012 Wiley-VCH Verlag & Co. KGaA (2012) ; 1-100

[100] N.Ghaemi,S.S.Madaeni,A.Alizadeh,H.Rajabi,P.Daraei,Preparation, characterization and performance of polyethersulfone/organically modified montmorillonite nanocomposite membranes in removal of pesticides, J. Membr. Sci.382(2011)135–147

[101] V.Vatanpour, S.S.Madaeni, R.Moradian, S.Zinadini, B.Astinchap, Fabrication and characterization of novel antifouling Nanofiltration membrane prepared from oxidized multiwalled carbon nanotube/polyethersulfone nanocomposite, J.Membr.Sci.375(2011)284– 294.

[102] M.P. Sun, Y.L. Su, C.X. Mu, Z.Y. Jiang, Improved antifouling property of PES ultrafiltration membranes using additive of silica-PVP nanocompositie, Ind. Eng. Chem. Res. 49(2010) 790-796

[103] Isa Karimzadeh et al., Superparamagnetic Iron Oxide (Fe3O4) Nanoparticles Coated with PEG/PEI for Biomedical Applications: A Facileand Scalable Preparation Route Based on the Cathodic Electrochemical Deposition Method., Advances in Physical Chemistry (2017)

[104] Han, L.F.; Xu, Z.L.; Cao, Y.;Wei, Y.M.; Xu, H.T. Preparation, characterization and permeation property of Al2O3, Al2O3–SiO2 and Al2O3–kaolin hollow fiber membranes. J. Membr. Sci. 2011, 372, 154–164

[105] Ma, Y.; Shi, F.; Wang, Z.; Wu, M.; Ma, J.; Gao, C. Preparation and characterization of PSf/clay nanocomposite membranes with PEG 400 as a pore forming additive. Desalination 2012, 286, 131–137

[106] Han, M.-J.; Nam, S.-T. Thermodynamic and rheological variation in polysulfone solution by PVP and its effect in the preparation of phase inversionmembrane. J. Membr. Sci. 2002,

202, 55–61

[107] Gohari, R.J., Lau, W.J., Halakoo, E., Ismail, A.F., Korminouri, F., Matsuura, T., Gohari, M.S.J., Chowdhury, M.N.K., 2015. Arsenate removal from contaminated water by a highly adsorptive nanocomposite ultrafiltration membrane. New J. Chem. 35, 8263–8272

[108] Li, Q., Xu, X.T., Cui, A., Pang, J.,Wei, Z., Sun, Z., Zhai, J., 2012. Comparison of two adsorbents for the removal of pentavalent arsenic from aqueous solutions. J. Environ. Manag. 98, 98–106